CRC Report No. A-121-1
& A-121-2

MEASUREMENT OF VOLATILE CHEMICAL PRODUCTS (VCPS) IN LOS ANGELES AND BIOGENIC VS. ANTHROPOGENIC VOC ANALYSIS DURING PEAK OZONE EVENTS IN THE SOCAB

Final Report

October 2022

COORDINATING RESEARCH COUNCIL, INC.
5755 NORTH POINT PARKWAY • SUITE 265 • ALPHARETTA, GA 30022

The Coordinating Research Council, Inc. (CRC) is a non-profit corporation supported by the petroleum and automotive equipment industries. CRC operates through the committees made up of technical experts from industry and government who voluntarily participate. The four main areas of research within CRC are: air pollution (atmospheric and engineering studies); aviation fuels, lubricants, and equipment performance; heavy-duty vehicle fuels, lubricants, and equipment performance (e.g., diesel trucks); and light-duty vehicle fuels, lubricants, and equipment performance (e.g., passenger cars). CRC's function is to provide the mechanism for joint research conducted by the two industries that will help in determining the optimum combination of petroleum products and automotive equipment. CRC's work is limited to research that is mutually beneficial to the two industries involved. The final results of the research conducted by, or under the auspices of, CRC are available to the public.

LEGAL NOTICE

This report was prepared by UC Davis as an account of work sponsored by the Coordinating Research Council (CRC). Neither the CRC, members of the CRC, UC Davis, nor any person acting on their behalf: (1) makes any warranty, express or implied, with respect to the use of any information, apparatus, method, or process disclosed in this report, or (2) assumes any liabilities with respect to use of, inability to use, or damages resulting from the use or inability to use, any information, apparatus, method, or process disclosed in this report. In formulating and approving reports, the appropriate committee of the Coordinating Research Council, Inc. has not investigated or considered patents which may apply to the subject matter. Prospective users of the report are responsible for protecting themselves against liability for infringement of patents.

Measurement of Volatile Chemical Products (VCPs) in Los Angeles
and
Biogenic vs. Anthropogenic VOC Analysis During Peak Ozone Events in the SoCAB

REPORT TO THE

Coordinating Research Council

Project # CRC A-121 and A-121-2

Prepared by:

Dr. Michael J. Kleeman
Dr. Thomas M. Young
Dr. Peter G. Green

Department of Civil and Environmental Engineering
University of California, Davis
One Shields Avenue, Davis, CA, 95616

October 5, 2022

DISCLAIMER

ACKNOWLEDGEMENTS

The analysis described in this report was partially conducted by graduate students, postdoctoral scholars, and research scientists with guidance from their faculty mentors. In several cases, these students and postdocs are the lead authors of individual chapters that will be submitted for publication in peer-reviewed journals. The student, postdoctoral scholar, and research scientist team consisted of the following individuals:

Shenglun Wu – Graduate Student, Department of Civil and Environmental Engineering, UC Davis

Chris Alaimo – Staff Spectroscopist Department of Civil and Environmental Engineering, and Graduate Student, Agricultural and Environmental Chemistry Graduate Group, UC Davis

Luann Wong – Staff Research Associate, Department of Civil and Environmental Engineering, UC Davis

The authors thank the members of the Technical Advisory Committee for their feedback and guidance during the project.

The authors thank Albert Dietrich at the South Coast Air Quality Management District for help with site preparation and access during sample collection.

TABLE OF CONTENTS

LIST OF TABLES

LIST OF FIGURES

LIST OF ACRONYMS

AVOC – anthropogenic volatile organic compounds
BTEX – benzene, toluene, ethylbenzenes and xylene
CARB – California Air Resources Board
CRC – Coordinating Research Council
CNG – compressed natural gas
CPF – conditional probability function
CTM – chemical transport model
DNPH - dintrophenylhydrazine
GC – gas chromatography
H/C – hydrogen to carbon ratio
IVOCs – intermediate volatility compounds
LC – liquid chromatography
LOD – limit of detection
LOQ – limit of quantification
MMP – mobile monitoring platform
MS – mass spectrometry
NAAQS – National Ambient Air Quality Standards
ND – not detected
NM- no measurement
NO_x – oxides of nitrogen
O_3 – ozone
PAC – project advisory committee
PAH – polycyclic aromatic hydrocarbon
ppbv – parts per billion by volume
PMF – positive matrix factorization
qTOF - quadrupole time-of-flight
RVP – Reid vapor pressure
SCAQMD – South Coast Air Quality Management District
SOA – secondary organic aerosol
SoCAB – South Coast Air Basin
SVOC – semi-volatile organic compound
TCD – thermal conductivity detector
TD – thermal desorption
UCD – University of California at Davis
US EPA – United States Environmental Protection Agency
VCP – volatile chemical product
VOC – volatile organic compound

ABSTRACT

Tropospheric ozone (O_3) is a criteria pollutant that is harmful to human health as well as the environment due to its strong oxidative properties. California continues to violate the health-based standards for O_3 concentrations, motivating continued efforts to control precursor emissions. Oxides of nitrogen (NO_X) and volatile organic compounds (VOCs) are the driving pollutants in the O_3 formation cycle. Recent studies using mobile smog chambers have determined that excess VOCs are present during peak O_3 events (NO_x-limited regime). The seasonal cycle of the excess VOC concentrations suggests that biogenic emissions may contribute significantly to O_3 formation in parts of California. A greater understanding of the sources of VOCs that contribute to ambient O_3 concentrations would enable the design of more efficient emissions control strategies.

VOC samples were collected at the Dearborn Reservoir monitoring site in the city of Redlands, CA, in parallel with mobile smog chamber measurements of O_3 sensitivity to NO_x and VOC perturbations. VOC measurements started on July 10, 2021, and ended on November 1, 2021, as part of the Re-Evaluating the Chemistry of Air Pollution in California (RECAP-CA) field campaign. Four Thermal Desorption (TD) tubes (1L, 1L, 3L, 7L) and one 2,4-dinitrophenylhydrazine (DNPH) tube (1L) were collected during each sampling event. All samples were collected in the morning hours between ~ 10 AM – 12 PM to characterize the air at the start of each daily photochemical cycle. VOC samples were analyzed for 213 target compounds using a combination of LC/MS and GC/MS techniques following a rigorous protocol of multi-point calibrations using authentic standards. A total of 95 VOC compounds were quantified at concentrations above detection limits over multiple days using this method. Major compound classes characterized by the measurements include halocarbons and volatile organics, aldehydes and ketones, alcohols and phenols, semi-volatile organic compounds, total organic silicon, and terpenes.

The majority of the VOC concentrations followed an expected log-normal concentration profile. Time trends were apparent in many VOC concentrations corresponding to seasonal temperature patterns, day-of-week patterns, and seasonal activity patterns. Terpenes underwent a seasonal cycle of declining concentrations as summer progressed to fall punctuated by high concentrations events that may be associated with the periodic cutting of grasses or hay. Compounds within the benzene/toluene/ethylbenzene/xylene (BTEX) category had both a day of week pattern and a seasonal pattern, suggesting that temperature strongly influenced evaporative emissions from motor vehicles. Several halogenated compounds and assorted volatile chemical products had markedly increased concentrations starting in the fall season when summer blend gasoline transitioned to winter-blend gasoline, and when classes had resumed at the nearby University of Redlands.

Positive Matrix Factorization (PMF) analysis identified eight VOC factors with preliminary source names recognized as (i) evaporation of liquid motor vehicle fuel, (ii) escape of vapors from the headspace of petroleum storage tanks, (iii) biogenics, (iv) volatile chemical products (VCPs) associated with siloxanes, (v) University and K12 institutional chemicals, (vi) halogenated solvents, (vii) methanol with contributions from gasoline and composting, and (viii) ethanol derived from VCPs. In order of decreasing importance, O_3 formation was most strongly

associated with the VCP (siloxane), biogenic, halogenated solvents, VCP (ethanol), and liquid fuel evaporation at the Redlands location. These associations do not reflect the direct O_3 formation potential for the VOCs measured in each factor, indicating that associations may be driven by underlying mechanisms.

1 INTRODUCTION

Tropospheric ozone (O_3) is a criteria pollutant that is harmful to human health as well as the environment due to its strong oxidative properties. Limits for O_3 concentrations designed to protect public health are specified by the National Ambient Air Quality Standards (NAAQS) and the California State Air Quality Standards. These target values are periodically revised based on the most recent and best available evidence describing the relationship between O_3 and human health. Despite extensive progress in the reduction of O_3 over the past four decades in California, the state continues to violate the health-based standards that have also decreased over that period. As a result, California continues to study strategies to better understand sources and formation mechanisms for O_3 in order to reduce concentrations.

Oxides of nitrogen (NO_X) and volatile organic compounds (VOCs) are the driving pollutants in the O_3 formation cycle and their concentrations can vary substantially depending on emissions from local sources such as motor vehicles, power plants, and the regional biosphere. O_3 pollution episodes typically occur during warm summer periods when the ultraviolet (UV) intensity (in Watts per square meter - W/m^2) is near its annual maximum. Population exposure to O_3 varies significantly based on location, time of day/year, and meteorological patterns. Reactive chemical transport models (CTM) that simulate all of these factors are often used to design effective O_3 mitigation strategies. In a typical design application, CTMs are first applied to a historical O_3 episode to ensure that they correctly reproduce the observed concentrations across the region of interest. Once satisfactory base-case model performance is attained, the emissions inputs to the models are reduced and the corresponding reduction in O_3 is simulated. There is often little or no ability to evaluate the accuracy of CTMs when calculating O_3 reductions in response to prospective emissions changes. Measured ratios of various photochemical indicator species can provide some confidence about the limiting precursors for O_3 formation but not the actual magnitude or the amount of O_3 reduction per unit of precursor reduction.

Recent studies carried out by the University of California, Davis in collaboration with the California Air Resources Board (CARB) and the Coordinating Research Council (CRC) have directly measured O_3 response to NO_x and VOC perturbations (Wu et al., 2022). Three parallel smog chambers equipped with UV lights were filled with ambient air at approximately 11 am each day. One chamber was used as a control for comparison to nearby monitors to verify that the system accurately represented atmospheric behavior. The second chamber was perturbed with +8 ppb addition of NO_2 while the third chamber is perturbed with +8 ppb addition of a VOC mixture (55% ethylene, 35% n-hexane, 10% xylenes) designed to represent urban VOCs. O_3 formation is compared within the three chambers after irradiation by UV lights with an intensity equivalent to a summer day in California.

Figure 1-1 shows the response of O_3 concentrations in Sacramento to NO_x and VOC perturbations as a function of the underlying O_3 concentrations. NO_x controls appear to be efficient during peak events, but this assumes that VOCs are 55% ethylene, 35% n-hexane, and 10% xylenes. The reactivity of the VOCs that drive the actual episode may be much different from those of the surrogate VOCs employed here. Detailed VOC measurements during peak episodes would help define VOC reactivity and differentiate between biogenic and anthropogenic sources, which could help to design optimized emissions control programs.

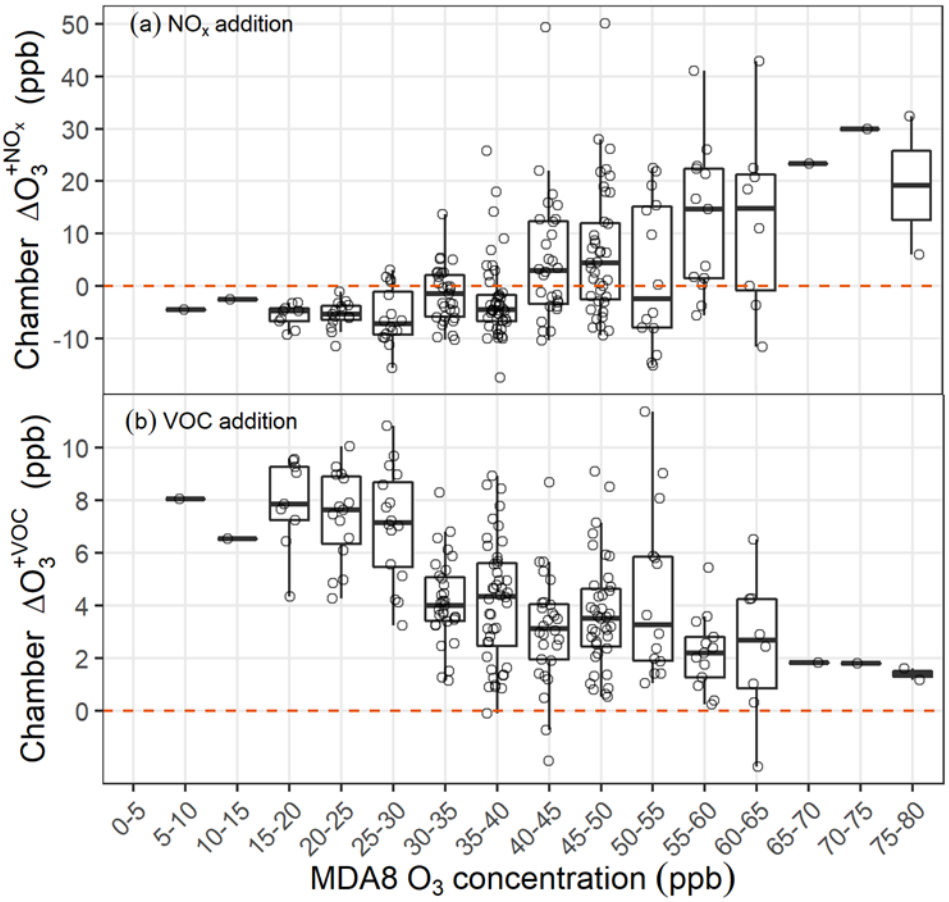

Figure 1-1: Boxplot of O_3 sensitivity to NO_x and VOC as a function of MDA8 O_3 concentration. Points indicate the data point in each range of MDA8 O_3 concentration.

The results are shown in Figure 1-1 to help identify the benefits of NO_x control, but further insights can be gained by looking at the time series of the measured response. Figure 2 illustrates the evolution of the O_3 response to NO_2 and VOC perturbations in the ambient atmosphere in Sacramento between April – December 2020. A strong weekend-weekday effect is obvious in the measurements consistent with past studies. NO_2 addition on weekends generally encourages higher O_3 formation because ambient concentrations of NO_x decrease on weekends when heavy-duty diesel engine activity is reduced.

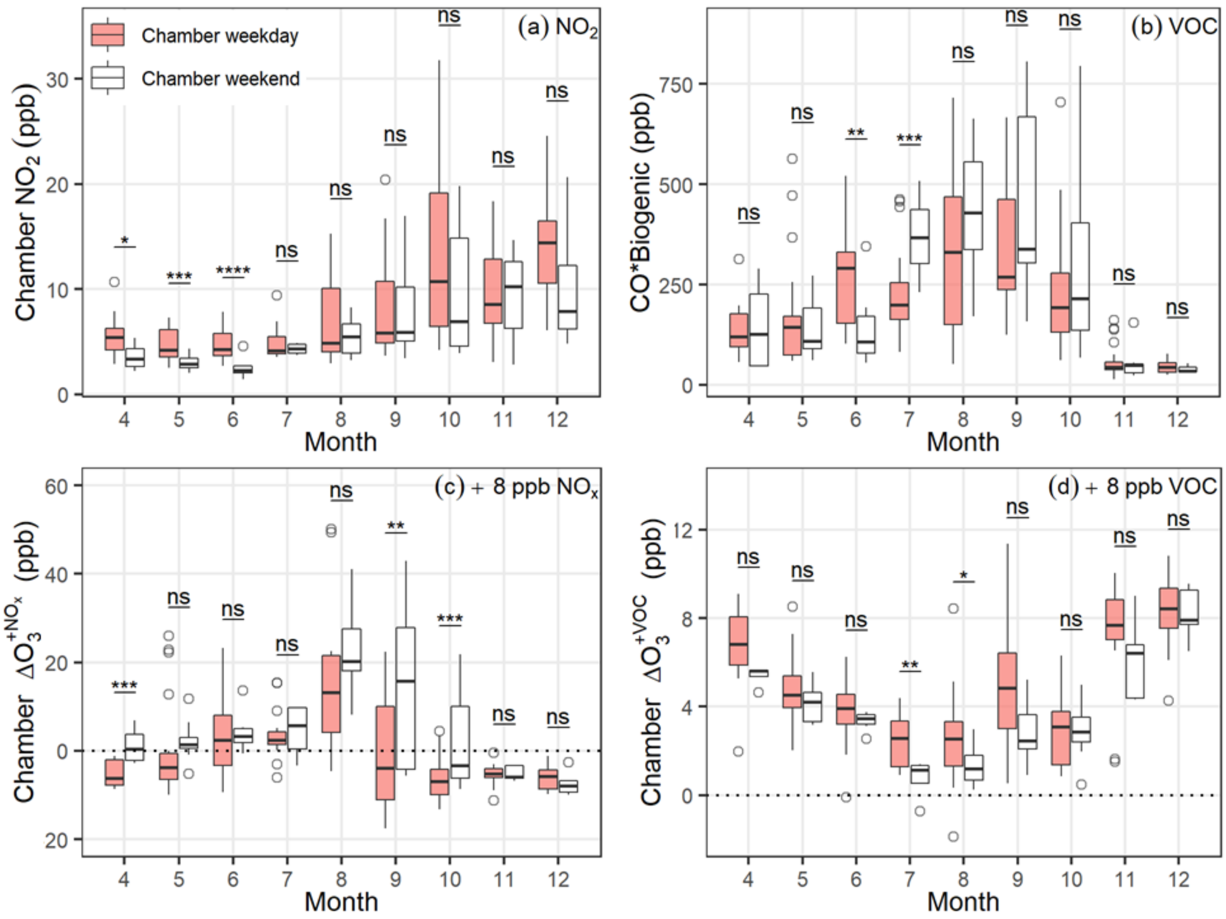

Figure 1-2: Weekday (solid box) and weekend (open box) monthly-average concentrations of NO2 and CO*biogenic (panels a, b), and $\boldsymbol{\Delta O_3^{+NO_x}}$ and $\boldsymbol{\Delta O_3^{+VOC}}$ (panels c, d) from April to December, 2020 after removing wildfire days. The stars above each box and whisker plot represent the significance of the weekday vs weekend difference. (*: p-value < 0.1, **: p-value < 0.05, ***: p-value < 0.01, ***: p-value < 0.001, ns (not significant): p-value >= 0.1) All ΔO3 values are relative to a base-case chamber operated under identical conditions. UV intensity was 50 W m-2 over an exposure time of 3 hrs.

In the context of the current project, the seasonal trends shown in Figure 1-2 over the entire study are just as interesting as the weekend-weekday effect. Sensitivity to NO_x increases and sensitivity to VOC decreases in the middle of the summer in the presence of constant chamber UV intensity. This pattern suggests that the reactivity of the ambient VOCs increased during the period April-August 2020 either (i) because VOCs were present at greater concentrations or (ii) because the VOC speciation changed to become more reactive. This pattern could be explained by the annual cycle of biogenic emissions. Increasing biogenic emissions between April – August 2020 would increase both the amount and reactivity of the ambient VOCs. O_3 source apportionment modeling conducted by the study team also suggests that biogenic VOCs are the dominant VOC category in California (funded separately by US EPA – results not shown). Taken together, these findings suggest that measurements are needed to characterize concentrations of biogenic VOCs relative to anthropogenic VOCs during summer months in California.

Biogenic VOCs emitted to the atmosphere include isoprene and numerous terpenes that can be simply described as molecules built from multiple isoprene units arranged in different structures. Isoprene reacts readily with OH, O_3, and NO_3, yielding an atmospheric lifetime of minutes to hours. Terpenes generally react more slowly in the atmosphere and so they may serve as more suitable tracers to help quantify the influence of biogenic VOCs on the atmospheric chemical reaction system.

2 OBJECTIVES

The objective of this project was to quantify organic compound concentrations at the Redlands monitoring site in Southern California for ~90 days over a full O_3 season. The measurement program focused on (i) halocarbons and other VOCs, (ii) aldehydes and ketones, (iii) semi-volatile organic compounds including polycyclic aromatic hydrocarbons, (iv) organic silicon (including siloxanes), and (v) biogenic compounds including terpenes. The terpenes react more slowly than isoprene and so they will serve as markers for biogenic influence in the measured air masses. The dataset will provide information that can be used to quantify the relative contributions to O_3 formation from biogenic vs. different anthropogenic sources such as volatile chemical products and mobile sources.

3 BACKGROUND

Long-term trends in NO_x and VOC concentrations have been studied in Los Angeles for more than 60 years. Measurements in Southern California confirm that ambient VOC concentrations decreased at an average rate of 7.5% yr^{-1}, while ambient NO_x concentrations decreased at an average rate of 2.6% yr^{-1} between the years 1980 to 2010 (Pollack et al., 2012; Warneke et al., 2012). Measurements in 2010 during the CalNex field campaign suggested that motor vehicles were still the dominant source of VOCs in the Los Angeles atmosphere (Parrish et al., 2016; Warneke et al., 2012). More recent VOC measurements during the pandemic period of 2020 showed that ambient VOC concentrations did not respond strongly to significant reductions in traffic volume (Van Rooy et al., 2021), suggesting that non-transportation sources may play an increasingly significant role in the residual VOC emissions inventory. The most likely candidate VOC categories are volatile chemical products (McDonald et al., 2018) and biogenic VOCs (Wu et al., 2022). Intermediate volatility compounds (IVOCs) are often discussed in the context of secondary organic aerosol (SOA) formation (Lu et al., 2020) but are generally not considered to be dominant contributors to O_3 formation. The current study attempts to interpret the time trends of VOC concentrations measured in summer 2021 in the context of these previous measurements.

4 METHODS

4.1 Aldehyde and Ketone Analysis

Airborne carbonyl compound concentrations, including those of methyl ethyl ketone and cyclohexanone, are determined using a modified version of the US EPA method TO-11 (U.S. Environmental Protection Agency, 1999b), "Determination of formaldehyde in ambient air using adsorbent cartridge followed by high-performance liquid chromatography." The method has been optimized for the analytical equipment and target compounds used here.

Air samples are drawn through an 8 x 115 mm 2,4-dintrophenylhydrazine (DNPH)-treated silica gel sorbent tube (SKC, Inc.) for 70 min, at a flow rate of 1 l/min, using an "Aircheck Sampler" personal sampling pump (SKC, Inc.) which is calibrated for a flow rate of 1 l/min using a MesaLabs Defender 510 dry sampling pump calibrator. Sorbent tubes remained sealed until sampling, and they were capped, labeled, and placed into a cooler immediately after sampling. Once transported back to the lab, it is stored in a 0 °C freezer until extraction. Sorbent tubes may be held at 0 °C for up to 30 days before being extracted. To extract the sorbent material, tubes are broken open and each section of the sorbent material is transferred to a labeled glass vial. Acetonitrile (1 ml) is added to each vial, which is then capped and allowed to sit for 30 min. The supernatant liquid is transferred to a labeled amber glass autosampler vial.

Sample analysis is carried out on an Agilent 1200 liquid chromatograph coupled with an Agilent 6530 quadrupole time-of-flight (qTOF) mass spectrometer. Separation is accomplished using a Restek Ultra C18 Column (5 µm, 250 x 4.6 mm). The injection volume is 10 µl and the LC gradient is 40 percent A (deionized H_2O with 1 mM CH_3COONH_4) and 60 percent B (ACN/H_2O, 95/5 v/v with 1 mM CH_3COONH_4) for 7 min, followed by a linear increase to 100 percent B at 20 min, hold at 100 percent B for 0.5 min. Each sample run includes a system blank, two sample blanks (1 set of sorbent tube extracts), calibration standards, and the samples. A multi-point calibration curve generated from the calibration standards (Sigma 47285-U TO-11 Standard Mix) is used to quantify the target compounds.

4.2 Volatile Organic Compound Analysis

Concentrations for all other organic species are determined using a modified version of the US EPA method TO-17 (U.S. Environmental Protection Agency, 1999a), "Determination of Volatile Organic Compounds in Ambient Air Using Active Sampling onto Sorbent Tubes." The method has likewise been optimized for this analytical equipment and the selected target compounds.

Air samples are drawn through an inert-coated stainless steel "Universal" thermal desorption tube (Markes International, Inc.) which is packed with a proprietary mixture of sorbents that maximizes trapping efficiency over a wide range of compound volatilities. Sample volumes of 1, 3, and 7 L are collected at a flow rate of 0.1 LPM using a Gillian LFS-113 low flow personal sampling pump, which is calibrated using a MesaLabs Defender 510 dry sampling pump calibrator. Tubes are kept sealed until just prior to sampling, and are immediately resealed once the sample has been collected. Capped tubes are kept cold (4 °C) until shipping to the laboratory from the sampling site, which occurred after every third sampling day; upon receipt at the laboratory, tubes are immediately analyzed.

Sample tubes are thermally desorbed using a Markes Unity 2 thermal desorption unit, which under a flow of helium (10 mL/min) heats the tube to 250 ˚C for 5 minutes, recollecting the sample onto a TO-17-specific cold trap. This trap is then rapidly heated to 280 ˚C, with the flow from the trap being transferred directly onto the analytical GC column.

Sample analysis is carried out on an Agilent 6890N gas chromatograph coupled with an Agilent 5973N single quadrupole mass spectrometer. Separation is achieved using an Agilent DB-VRX column (60 m x 0.25 mm, 1.4 µm film thickness) using helium as the carrier gas. The GC oven is held at 35 ˚C for 5 minutes, before ramping up to 250 ˚C at 7.5 ˚C/min, with a final hold time of 10 minutes.

Multi-point calibration curves prepared using analytical standards are used to quantify the target analytes in each compound group. TO-15 compounds (volatile halocarbons & VOCs), C1-C3 alcohols, and C3-C5 hydrocarbons are quantified using fixed-concentration gas standards (Air Liquide, Inc.) drawn through a series of thermal desorption tubes for varying lengths of time to build the calibration curve. Other analytes, including fragrance compounds, terpenes, siloxanes, glycols, glycol ethers, and other semi-volatiles are quantified by creating a liquid dilution series for each compound group and then loading 1 µl of these standards onto thermal desorption tubes using a calibration solution loading rig (Markes International, Inc.)

4.3 Quality Control and Detection Limits

Each sample run includes a tube blank to assess possible carry-over between samples and any other potential sources of interference affecting the detectability and quantification of target compounds. Each run also includes quality control (QC) checks in the form of single-point standards periodically run to confirm instrument performance. Following each instrument run, peaks are initially detected and integrated (Agilent Quantitative Analysis v.B09) based on selected quantifier and qualifier ions for each compound. Each target compound peak integrated by the quantitative analysis software is manually inspected to assess peak shape and to ensure that the ion count is at least 10 times the baseline noise in the extracted ion chromatogram of the quantifier ion for that sample. Consequently, every compound with a reported concentration is safely above the limit of detection (LOD), which is typically defined as 3x the baseline noise, for that compound in the particular sample being examined. These sample-specific LODs will vary from sample to sample based on both sample-specific and analytical run-specific factors. To support comparisons with previous work, a Lowest Limit of Detection (LLOD) is reported for each compound, which is calculated as one-third of the lowest estimated concentration for that compound in any sample. The limit of quantification (LOQ) for each compound at each sampling volume employed is derived by dividing the compound mass present in the lowest reliably detected calibration standard by the gas volume sampled (1L, 3L, or 7L). Consequently, the LOQ is expected to decrease as the sampling volume increases. When compounds were detected only in the tubes sampled using higher volumes, only these samples were used to produce average concentration values.

All data in the report were reviewed to ensure that they met the project's quality control guidelines. If they did not, analyses were repeated (consistent with holding time limitations) or other necessary corrective actions were taken. In some cases, these steps still did not produce acceptable data; results for these samples are listed as "no measurement" (NM).

4.4 PMF analysis

The Positive Matrix Factorization (PMF) receptor model is widely used for the source apportionment of ambient air samples. Past studies have used PMF analysis to quantify source contributions to airborne particle matter (PM) (see for example Kim et al., 2004; Zhang et al., 2011) and VOCs (see example Brown et al., 2007; Guha et al., 2015; He et al., 2019; Ling et al., 2011; Simpson et al., 2020). In the present study, PMF is used to identify sources of VOC species at the Redlands monitoring site and to identify associations between O_3 formation and sources of VOCs.

The PMF calculation requires an input data matrix X with dimensions m×n, in which m represents the number of samples, and n represents the number of chemical species measured in each sample. In this study, m is the total number of sampling days and n is the number of selected VOC species. Row i stores the concentrations of all VOC species measured on day "i", while column j stores the time series of concentrations for species "j". The PMF model solves the chemical mass balance (Equation 1) between measured species concentrations and source profiles. In Equation (1), p represents the number of contributing factors, G represents the factor contribution, F represents the factor profile, and E represents the residual in the calculation. The goal of the PMF calculation is to find the optimal non-negative G and F matrices from input matrix X.

$$x_{ij} = \sum_{k=1}^{p} g_{ik} \times f_{kj} + e_{ij} \qquad (1)$$

Optimal solutions are obtained by minimizing the value of Q defined by Equation (2)

$$Q = \sum_{i=1}^{n} \sum_{j=1}^{m} [\frac{x_{ij} - \sum_{k=1}^{p} g_{ik} f_{kj}}{\sigma_{ij}}]^2 \qquad (2)$$

where σ_{ij} represents the uncertainty for each species in each sample. The algorithm used to set the values of the input data is described below:

$$x_{ij} = measured\ concentration\ of\ species\ j\ on\ day\ i\ \ (x_{ij} > LOD) \qquad (3)$$
$$x_{ij} = LOD/2\ \ (x_{ij} < LOD) \qquad (4)$$
$$x_{ij} = geometric\ mean\ of\ concentration\ \ of\ species\ j\ \ (x_{ij} =\ missing\ value) \qquad (5)$$
$$\sigma_{ij} = \mu_{ij} + LOD/3\ \ \ (for\ determined\ value) \qquad (6)$$
$$\sigma_{ij} = LOD \times 5/6\ \ \ (x_{ij} < LOD) \qquad (7)$$
$$\sigma_{ij} = 4 \times geometric\ mean\ of\ concentration\ \ of\ species\ j\ \ (x_{ij} =\ missing\ value) \qquad (8)$$

where x_{ij} is the concentration of species j on sample day i; LOD is the limit of detection (see Section 4.3); μ_{ij} is the analytical uncertainty of species j on sample day i; σ_{ij} is the uncertainty used in PMF calculations for species j on sample day i.

5 SITE DESCRIPTION

5.1 Location

VOC samples were collected at the Dearborn Reservoir monitoring site (34.059671, -117.147304) maintained by the South Coast Air Quality Management District (SCAQMD) in the city of Redlands, CA starting on July 10, 2021, and ending on November 1, 2021. Residential neighborhoods and a mixture of commercial and industrial land use surround the monitoring site. The possible anthropogenic sources nearby include two major highways, two airports, several fueling stations, a fuel storage depot, several dry cleaners, a university and two K-12 schools, commercial stores in downtown Redlands, a shopping center, and residences (see map in Figure 5-1:). The population density is higher in the west direction (downtown Redlands) and northwest direction (San Bernardino). A variety of trees and shrubs around the monitoring site and nearby residences may contribute to the biogenic emissions.

Figure 5-2 shows all the facilities inside the Dearborn Park monitoring site during the study period. The UCD mobile smog chamber and the CARB Mobile Monitoring Platform (MMP) (onsite starting August 13, 2021) were parked beside the SCAQMD monitoring station. Routine measurements reported by SCAQMD include O_3, NO_x, PM_{10}, and temperature. VOC samples were collected using sorbent tubes beside the inlet of the UCD mobile smog chamber at an elevation of 2 m above the ground. The trailer housing the UCD mobile smog chamber contained two gas cylinders (NO_x and a VOC mixture including ethylene, n-hexane, and m-xylene), one O_3 monitor, one NO_x monitor, one NO_y monitor, and one portable air conditioner. The exhaust from all monitors was vented 3 m downwind from the VOC sample collection point. The CARB MMP contains one PTR-MS, one NO_x monitor, and one portable air conditioner. Vehicle traffic inside the fenced site was minimal, consisting mostly of a single parked UCD vehicle and occasionally vehicles from SCAQMD or the Redlands Water Department parked adjacent to the monitoring trailer. Vehicle activity adjacent to the monitoring site was recorded in a daily log.

VOC sample collection started each day when the UCD mobile smog chambers began to fill with ambient air at approximately 10 am. Four Thermal Desorption (TD) tubes (Markes Universal Sorbent Tube) and one 2,4-dinitrophenylhydrazine (DNPH) tube (SKC, Inc.) were collected during each sampling event. Ambient air was drawn through TD tubes at a flow rate of 0.1 LPM using a Sensidyne LFS-113 pump. Four different TD tubes were sequentially collected at different volumes (1L, 1L, 3L, 7L). Ambient air was drawn through DNPH tubes using a SKC universal sampling pump at a flow rate of 1 LPM concurrently with the collection of the 7L TD tube. Both sampling pumps were calibrated using a DryCal flow meter and adjustments were made as needed to maintain target flow rates. Activities within 6 m of the sample collection point were minimized during active sample collection to avoid contamination.

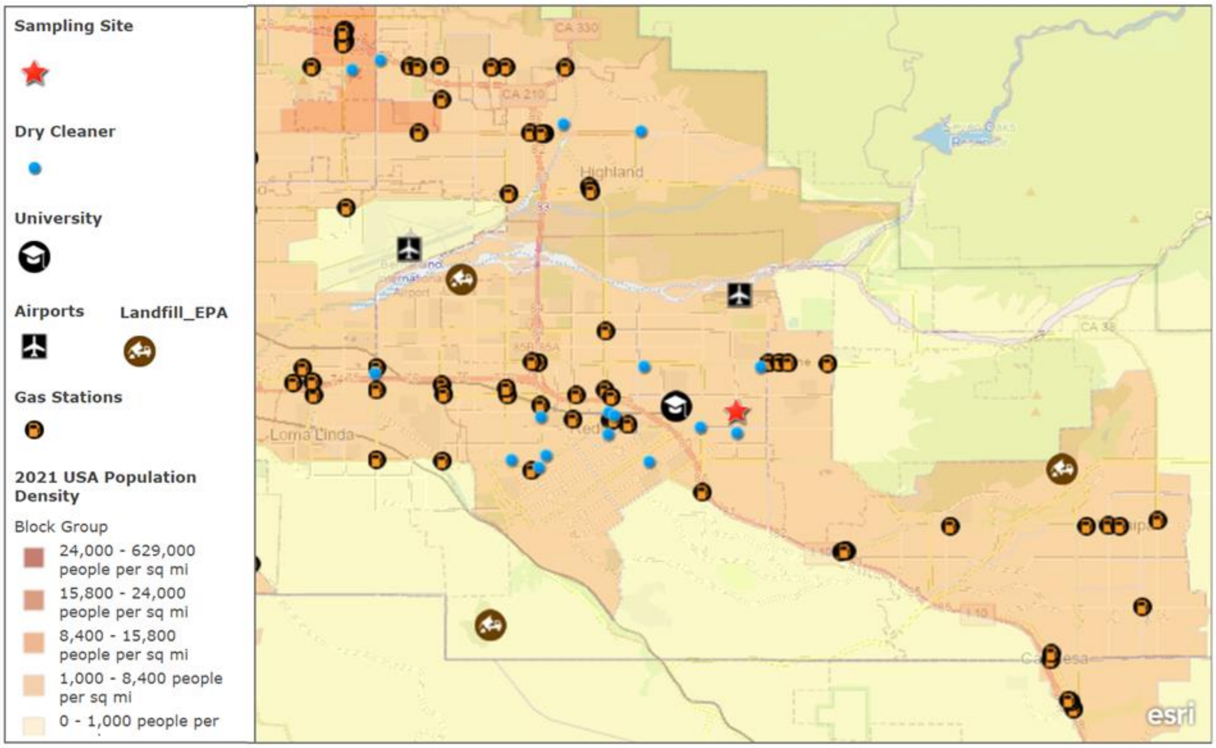

Google | Map data © OpenStreetMap contributors, Microsoft, Facebook, Inc. and its affiliates, Esri Community Maps contributors, Map layer by Esri | Esri, US Census Bureau, Infogroup | © OpenStreetMap contributors | Federal Aviation Administration (FAA), National Transportation Atlas; Esri

Figure 5-1: Location of the VOC measurement site in Redlands, CA. Locations of possible VOC sources including dry cleaners, gas stations, and universities are labeled on the map. Map color corresponds to population density.

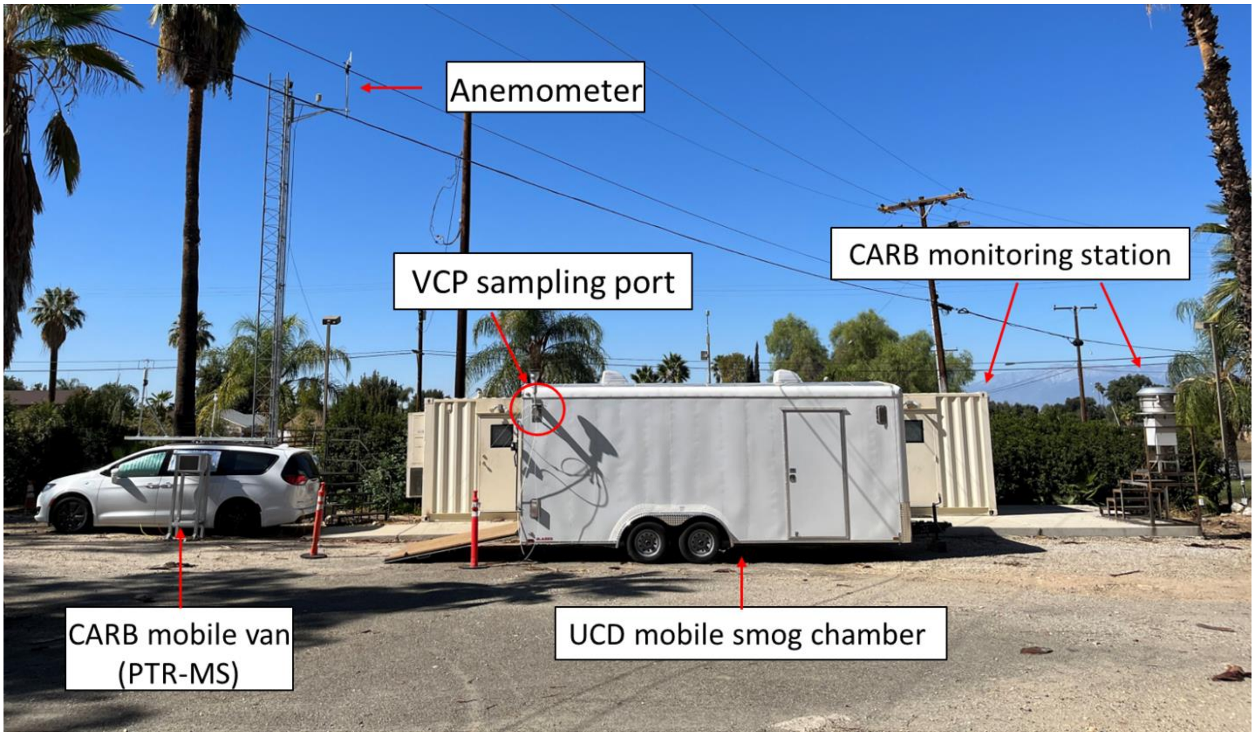

Figure 5-2: Overview of the VOC measurement site in Redlands, CA.

5.2 Meteorology

Figure 6-14 shows the measured time series of temperature and relative humidity (RH) at the SCAQMD monitoring site. Peak daily temperatures declined noticeably starting in mid-September during the transition to the fall season. Corresponding RH increased over this time period. Temperature is expected to affect emissions of biogenic compounds, evaporative emissions from motor vehicles, and fugitive emissions from landfills (via a corresponding change in pressure).

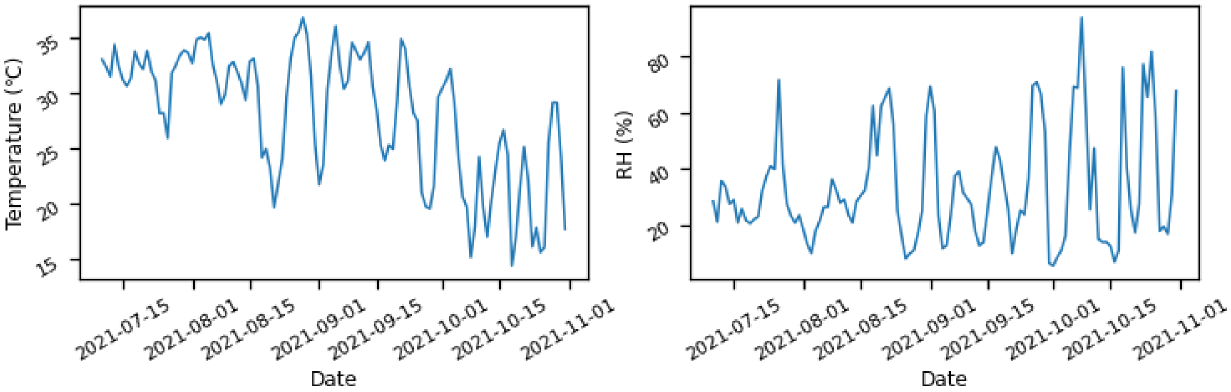

Figure 5-3: Time series of measured temperature and relative humidity. All data from the SCAQMD monitoring site.

Wind speed and wind direction data were collected at the SCAQMD monitoring site in Redlands hourly. Figure *5-4* shows the time series of hourly wind speed and direction between 10 AM – 12 PM every day during the study period (July 10 – October 31, 2021). The wind direction in the morning was mostly from the West (W) to Northwest (NW) direction. A few days with winds from the South (S) occurred mainly in October. The map of the sampling site (Figure 5-1) shows that downtown Redlands, a highway, and the University of Redlands are located to the west of the measurement site. The commercial stores, traffic sources, and emissions from the university all have the potential to contribute to measured VOC concentrations at the monitoring site. Long-range transport of emissions and their reaction products from cities further west could also impact the sampling site, including from downtown Los Angeles.

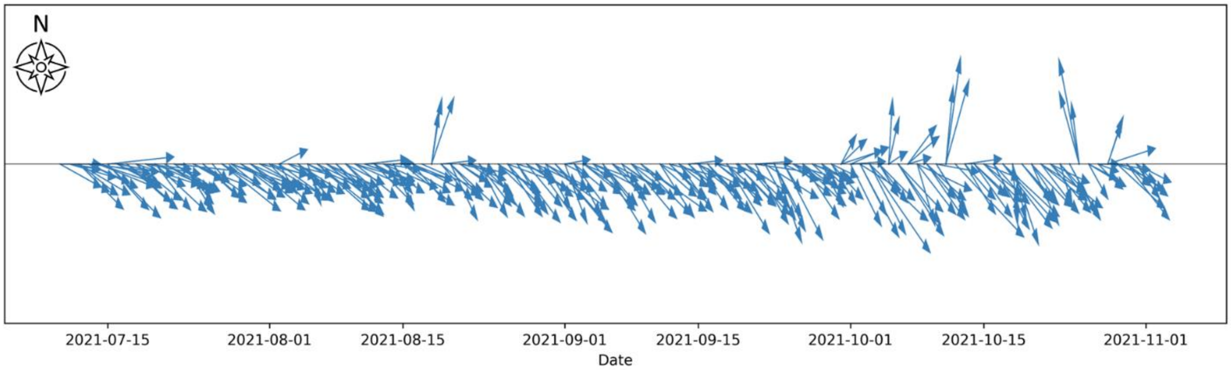

Figure 5-4: Time series of wind profile (wind direction + wind speed). The direction of each arrow shows the wind direction. The length of arrow indicates wind speed. All data representative of times between 10 AM – 12 PM every day from July 10 – October 31, 2021.

6 MEASUREMENT RESULTS

6.1 Overview

The results shown in the following sections include measurements from the UCD VOC sampling program, the UCD mobile smog chamber, and the SCAQMD monitoring station in Redlands. All of the VOC compounds measured using TD tubes (except alcohols) were quantified for three different sample volumes (1L, 3L, 7L). The weighted average concentration across all sample volumes was calculated for these compounds and reported as the daily concentrations. The combined sample volumes characterize the ~2 hr period used to fill the UCD mobile smog chambers. Concentrations measured in each sample volume were compared to verify that breakthrough did not occur since this would bias the calculated average concentration. All the non-detected measurements (reported by 0 or ND) were ignored when calculating the average. Alcohol concentrations were reported based on measurements from a single daily sample (1L TD tube). Likewise, carbonyl concentrations were quantified based on measurements from a single daily sample (DNPH tube). All measurements reported in the following section characterize the atmosphere during the hours ~ 10 am to 12 pm when UCD mobile smog chambers were being filled.

Species with statistically significant seasonal trends were identified using hypothesis tests applied to the results of the least squares linear regression with time as the independent variable and concentration as the dependent variable. Each test used a null hypothesis that the slope of the regression line was zero. Species with a significant seasonal trend had p-values less than 0.05. A second hypothesis test was conducted to identify species with higher concentrations in the fall (October). Concentrations of several compounds increased during this month, possible due to shifting meteorological patterns, shifting activity patterns, and/or shifting emissions patterns. The average concentration of each compound before October was compared to the average concentration in October, with a null hypothesis that the two means were equal. Tests yielding p-values less than 0.05 identified species with higher concentrations in October. Table S1 (in SI) shows the results from the two hypothesis tests.

6.2 Halocarbons and Volatile Organics Analysis

Figure 6-1 shows the measured time series of alkane concentrations. Many of these compounds are prevalent in gasoline. Concentrations for several alkanes (2-Methyl pentane, Heptane, Isobutane, Isopentane) had decreasing seasonal concentration trends throughout the study period, possibly due to generally decreasing temperatures leading to reduced evaporation losses from motor vehicles and fueling operations (3 out of 4 compounds have a significant correlation with temperature described in Section 7.4). Conversely, concentrations of butane are significantly higher in October than in previous months. This may correspond to the transition between summer blend gasoline and winter blend gasoline in the SoCAB (California Energy Commision, 2020). Winter blend gasoline usually replaces summer blend gasoline in the Kinder-Morgan distribution pipeline 1~2 months before Nov 1 every year. Compared with summer blend gasoline, winter blend gasoline has higher Reid Vapor Pressure (RVP) and contains higher concentrations of butane (California Energy Commision, 2020).

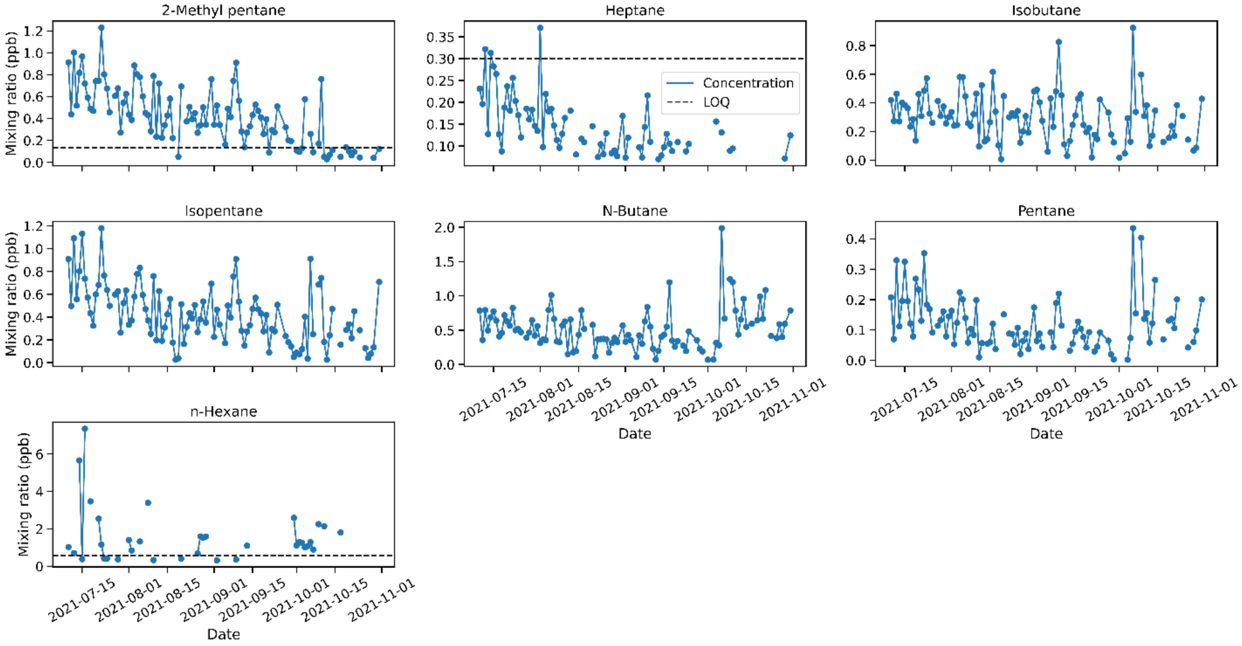

Figure 6-1: Time series of measured alkane concentrations.

Figure 6-2 displays the time series of alkene concentrations measured during the study period. All reported measurements are well above LOD and the authors believe that the time series of each displayed compound contains meaningful information, possibly even below the indicated value of the LOQ. Seasonal trends are apparent for cis-2-pentene (P value < 0.05). Increased fall concentrations are apparent for propylene. Although pentane also increases in the fall season (Figure 6-1), the day-to-day increase in pentane and propylene concentrations are not synchronized. Multiple factors could cause increasing concentrations in the fall, including resumption of university and K-12 activities, increased prevalence of winds from the Southern direction, or seasonal changes to the gasoline blend.

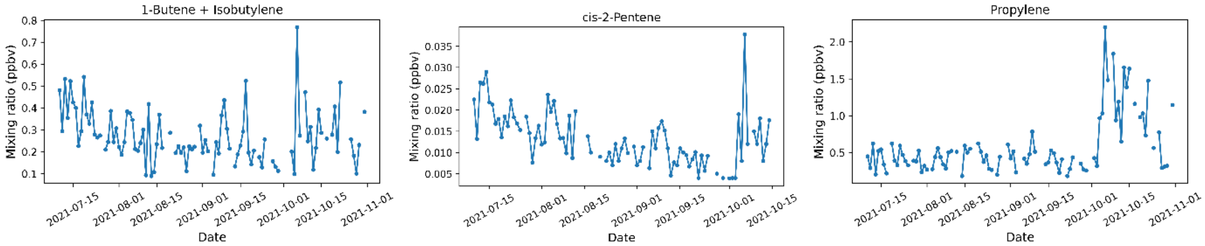

Figure 6-2: Time series of measured alkene concentrations.

Figure 6-3 displays the time series of aromatic compound concentrations. Strong seasonal trends (P value < 0.05) are apparent for benzene, ethylbenzene, toluene, and xylenes (the four compounds traditionally discussed together as “BTEX”). The seasonal pattern for these compounds is qualitatively consistent with higher evaporative losses from motor vehicles in the middle of summer followed by decreasing evaporative losses as temperatures decrease in the fall season. These trends will be discussed in Section 7.4 below. Increasing concentrations during the fall season are not apparent for BTEX compounds, perhaps because their concentrations are consistent in summer blend and winter-blend gasoline. California sets limits for aromatics (25% by volume) and benzene (0.8% by volume) in Phase 3 Reformulated Gasoline (CaRFG3) (Karavalakis et al., 2015). There is no evidence that the aromatic content of gasoline changes strongly between summer and winter blends. A previous study (Gentner et al., 2009) showed that the toluene and xylene concentration in the headspace vapor of liquid gasoline changes by less than 10% between summer and winter blends.

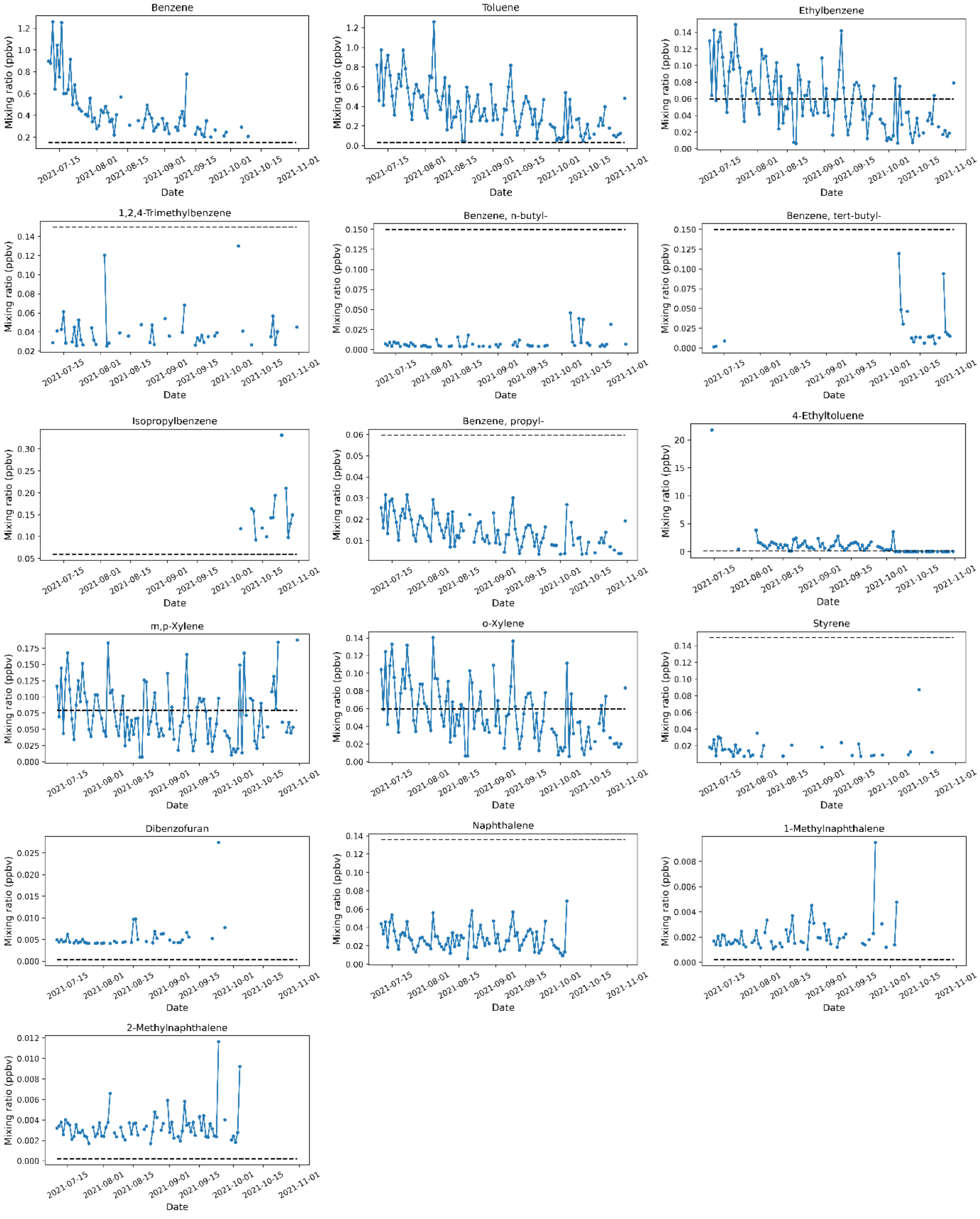

Benzene

Toluene

Ethylbenzene

1,2,4-Trimethylbenzene

Benzene, n-butyl-

Benzene, tert-butyl-

Isopropylbenzene

Benzene, propyl-

4-Ethyltoluene

m,p-Xylene

o-Xylene

Styrene

Dibenzofuran

Naphthalene

1-Methylnaphthalene

2-Methylnaphthalene

Figure 6-3: Time series of measured aromatic concentrations.

Figures 6-4 and 6-5 display the time series of halogenated compound concentrations. These compounds are used in cleaning solvents and formerly as refrigerants (Scheutz et al., 2000). Halogenated compounds may be released as fugitive emissions from landfills that contain a variety of legacy devices. Carbon tetrachloride, chloroform, and dichloromethane concentrations follow a seasonal pattern with decreasing concentrations corresponding to decreasing temperatures. Landfill gas is emitted into the atmosphere from soil due to pressure and concentration gradients. Lower atmospheric pressure in hotter seasons may cause higher pressure gradients leading to higher landfill gas emissions. Increasing evaporative losses from landfills are expected at hotter temperatures (Kumar et al., 2011; Scheutz et al., 2000). Dichloro-benzene (1,2- and 1,4-) concentrations show a clear increase in the fall season. These trends may be associated with increased fall activity on the campus of the University of Redlands or nearby K-12 institutions, or a higher prevalence of winds from the South during the fall time period.

Trichlorofluoromethane (CFC-11) and dichlorodifluoromethane (CFC-12) were banned under the Montreal Protocol signed in 1987. Measurements of CFC-11 have been made for decades to better understand the behavior of the stratospheric ozone hole (Montzka et al., 2018). The global mean CFC-11 concentration has declined over the last several decades. The global mean CFC-11 concentration in 2021 was around 220 ppt. CFC-11 concentrations in this study range between 200 ~ 500 ppt. The CFC-11 background level could be two times higher than averaged summer concentrations. Dichlorodifluoromethane (CFC-12) was typically co-produced with CFC-11 when production of both was allowed (Park et al., 2021). A past study (New Jersey Department of Environmental Protection, 2016) measured background CFC-12 concentrations of approximately 600 ppt in urban and suburban areas in New Jersey. The concentration of CFC-12 in this study is mostly between 400 – 700 ppt, which is comparable to background levels.

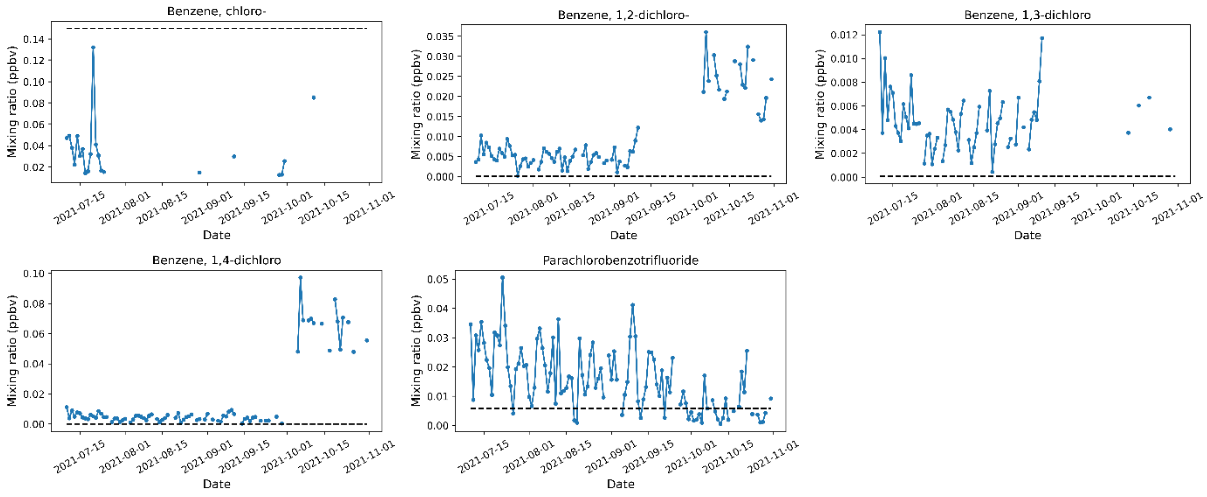

Figure 6-4: Time series of measured halogenated aromatic concentrations.

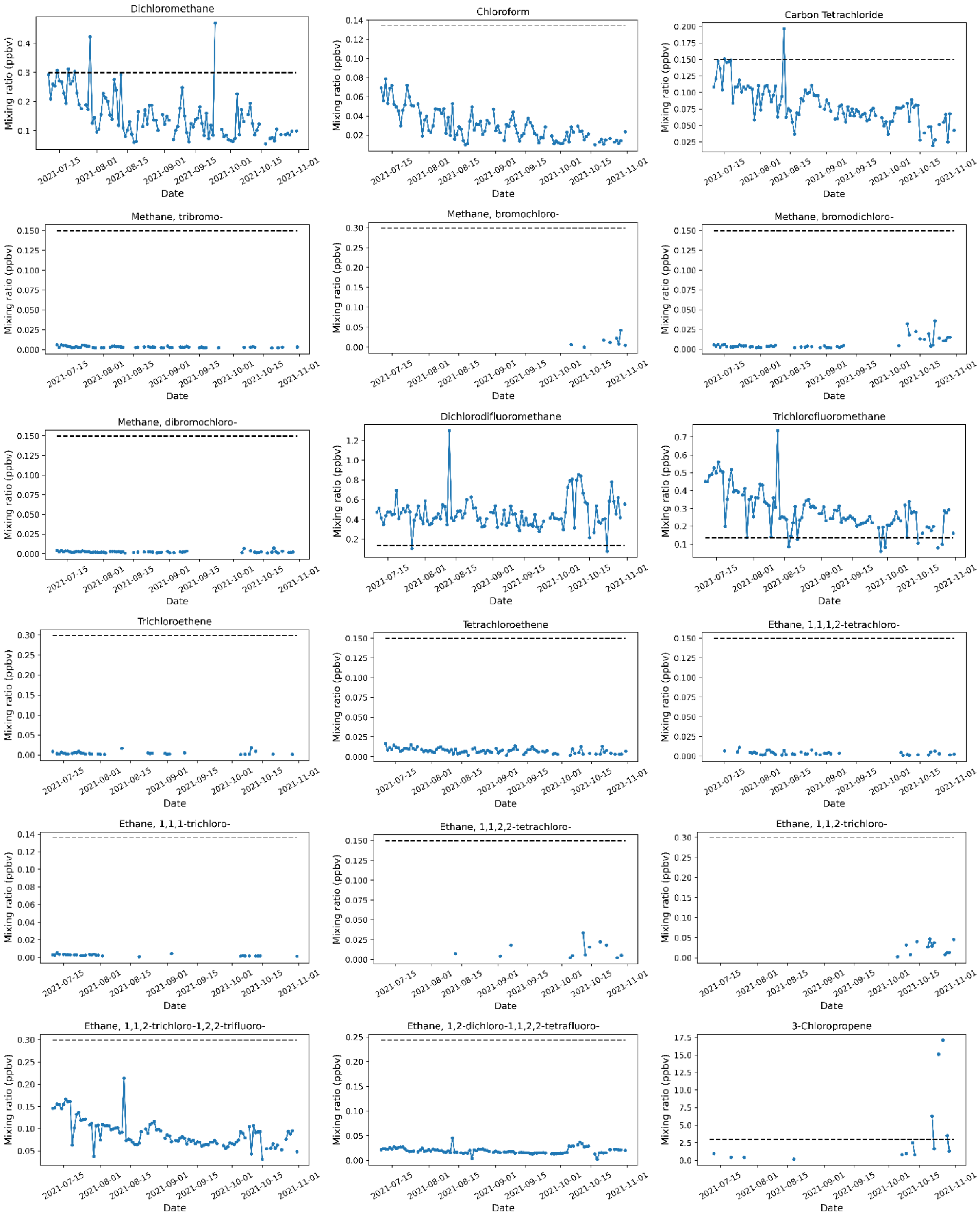
Dichloromethane
0.1
0.2
0.3
0.4
Chloroform
0.02
0.04
0.06
0.08
0.10
0.12
0.14
Carbon Tetrachloride
0.025
0.050
0.075
0.100
0.125
0.150
0.175
0.200
Methane, tribromo-
Methane, bromochloro-
Methane, bromodichloro-
Methane, dibromochloro-
Dichlorodifluoromethane
Trichlorofluoromethane
Trichloroethene
Tetrachloroethene
Ethane, 1,1,1,2-tetrachloro-
Ethane, 1,1,1-trichloro-
Ethane, 1,1,2,2-tetrachloro-
Ethane, 1,1,2-trichloro-
Ethane, 1,1,2-trichloro-1,2,2-trifluoro-
Ethane, 1,2-dichloro-1,1,2,2-tetrafluoro-
3-Chloropropene
0.0
2.5
5.0
7.5
10.0
12.5
15.0
17.5
Mixing ratio (ppbv)
Date
2021-07-15
2021-08-01
2021-08-15
2021-09-01
2021-09-15
2021-10-01
2021-10-15
2021-11-01

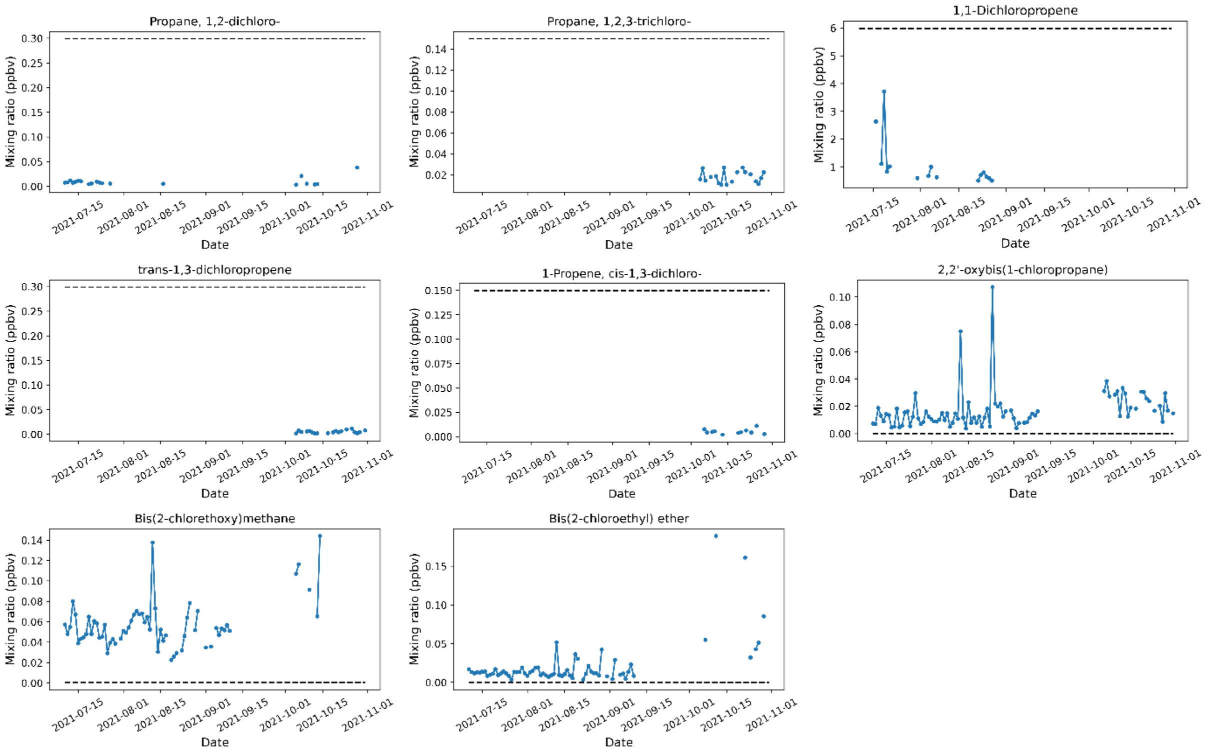

Figure 6-5: Time series of measured halogenated (non-aromatic) concentrations.

6.3 Aldehydes and Ketones Analysis

Figure 6-6 displays the time series of ketone concentrations, while Figure 6-7 displays the time series of aldehyde concentrations. These oxygenated compounds are produced by secondary atmospheric reactions, with minor contributions from primary emissions. There is little evidence of seasonal trends in most of the measured aldehyde and ketone concentrations, but there is a notable increase (p-value < 0.05) in butyraldehyde, benzaldehyde, isovaleraldehyde, and hexaldehyde concentrations during the fall season, suggesting that the increase in primary emissions noted in previous sections cascades into a corresponding increase in the production of oxygenated compounds in the atmosphere. As discussed previously, this may be related to the transition between summer blend and winter-blend gasoline, a shift in wind patterns, or the resumption of classes at nearby educational institutions.

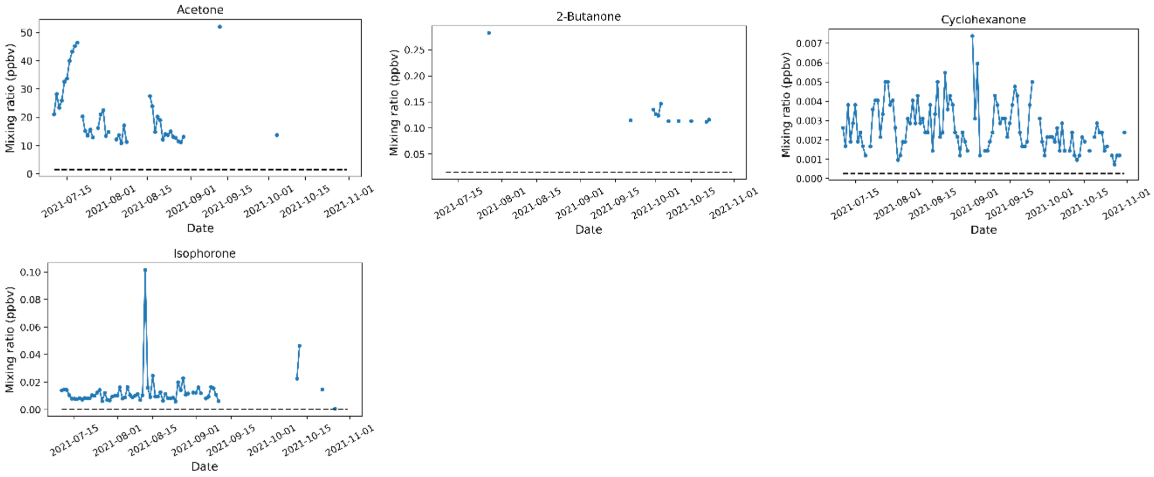

Figure 6-6: Time series of measured ketone concentrations.

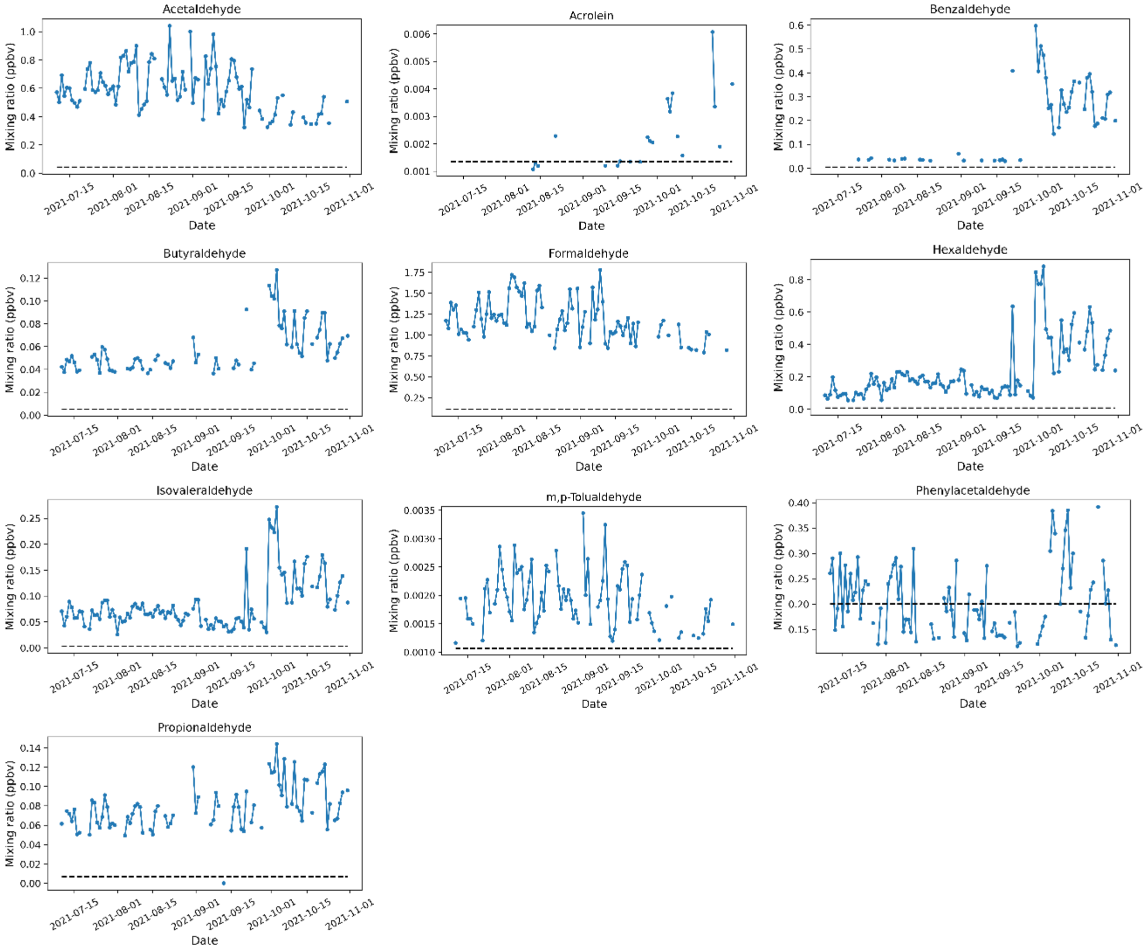

Figure 6-7: Time series of measured aldehyde concentrations.

6.4 Alcohols and Phenolic Compounds

Figure 6-8 displays the time series of measured alcohol and phenolic compounds. Ethanol followed a seasonal pattern of decreasing concentrations with temperature. Methanol concentrations exhibited periodic increases lasting 3-5 days on top of a relatively stable background level. This time pattern suggests the presence of an intermittent source. One possible example could be periodic cutting of tall grass or hay that is then left to dry. Phenolic compounds display mostly random behavior during the study period.

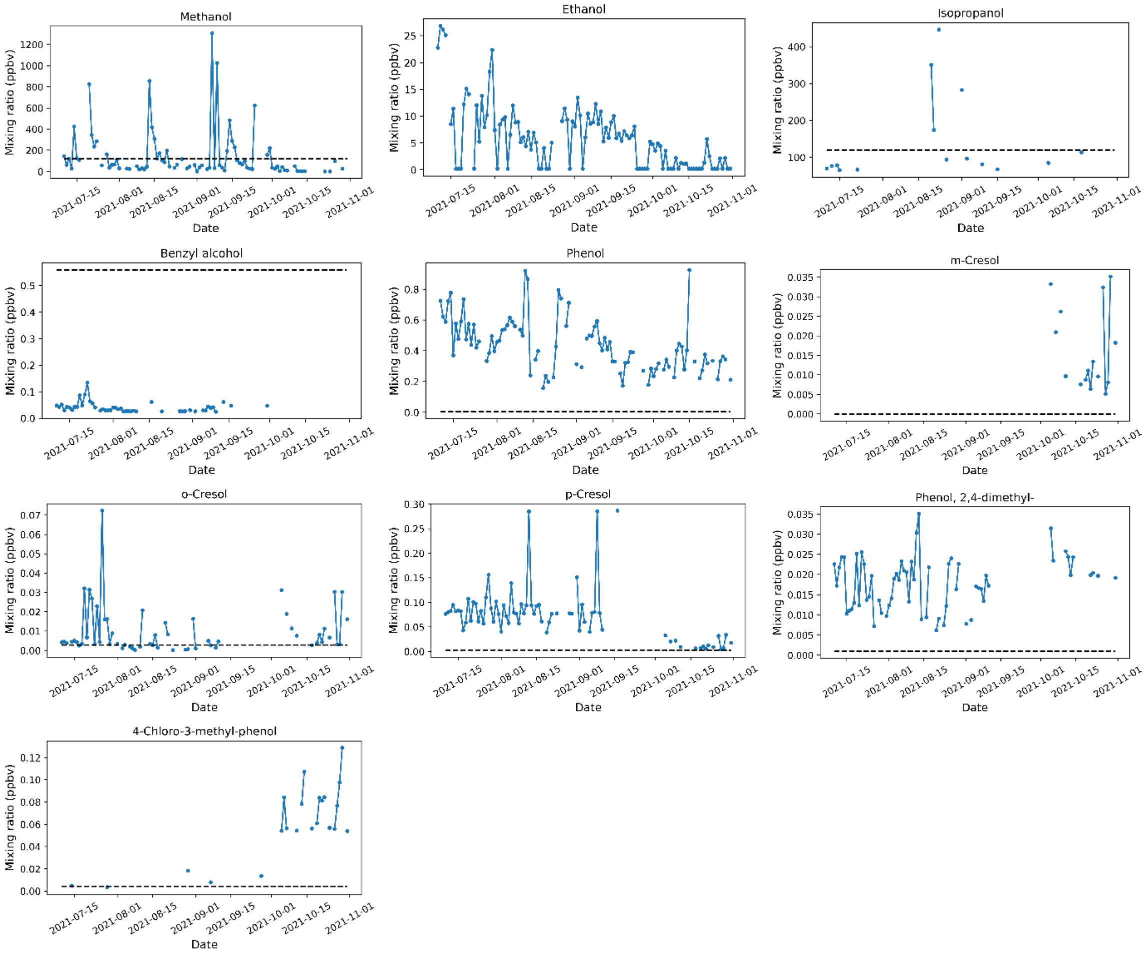

Figure 6-8: Time series of measured alcohol and phenol concentrations.

6.5 Semi-volatile Organic Compounds Analysis

Figure 6-9 displays the time series of ester concentrations. Esters can be emitted directly to the atmosphere or they can form through atmospheric chemical reactions. Diethylphthalate is one of the few compounds that displays a pattern of consistently increasing concentrations over the entire study period. This compound is used during the production of plastics, insecticides, cosmetics, and aspirin.

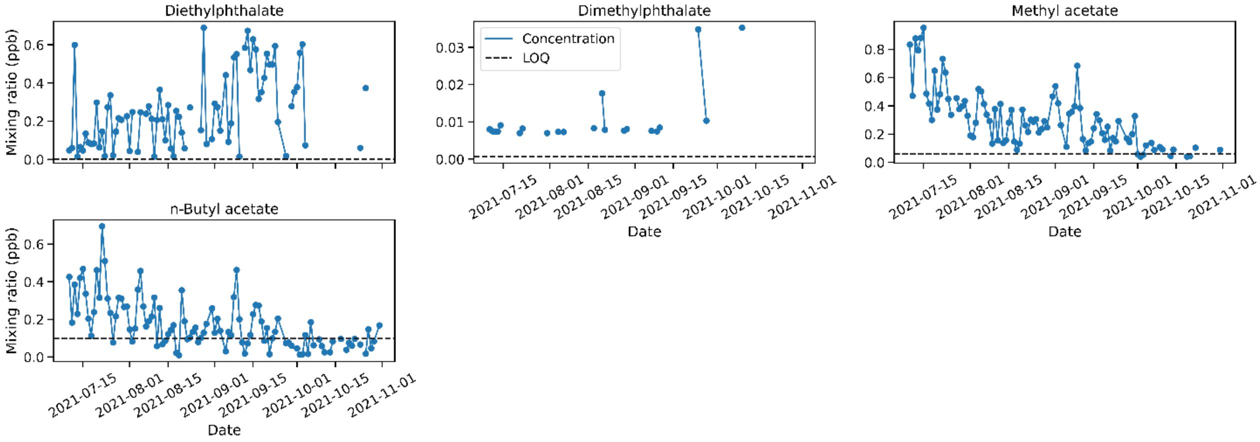

Figure 6-9: Time series of measured ester concentrations.

Figure 6-10 displays the time series of measured concentrations for VOCs containing nitrogen. Concentration patterns generally appear to be randomly distributed with the exception of increased concentrations of N-nitrosodimethylamine in the fall.

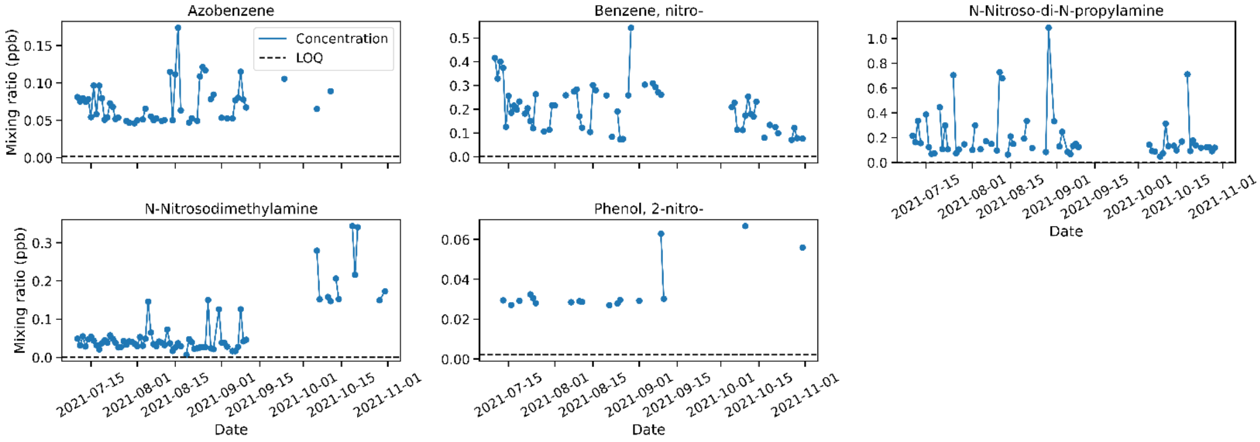

Figure 6-10: Time series of measured nitrogen-containing VOC concentrations.

6.6 Total Organic Silicon Analysis

Figure 6-11 displays the time series of measured siloxane concentrations. Only two siloxanes were detected during the study period. The D5 siloxane (decamethylcyclopentasiloxane) is used in personal care products, while the D4 siloxane (octamethylcyclotetrasiloxane) is used in insecticides. No trends are apparent in the D5 concentrations, while the D4 concentrations are only detectable in the fall. Increased fall concentrations may be related to resumption of classes at nearby educational institutions or a shift in wind direction. The different time trends for D4 and D5 siloxanes suggests these compounds are emitted by different sources.

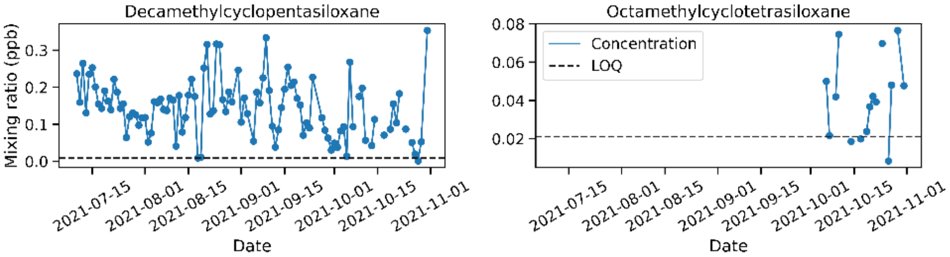

Figure 6-11: Time series of measured siloxane concentrations.

6.7 Terpenes

Figure 6-12 displays the time series of measured terpene concentrations. Limonene concentrations were sporadically above detection limits, but concentrations were notably higher in the fall. Increased fall concentrations may be related to a shift in wind direction or the resumption of classes at nearby educational institutions. Limonene is used as a flavoring in foods and beverages, and as an ingredient in water-free hand cleansers. p-Isopropyl Toluene (P-cymene) concentrations generally followed a decreasing seasonal concentration trend punctuated by periodic peak events lasting for a single day.

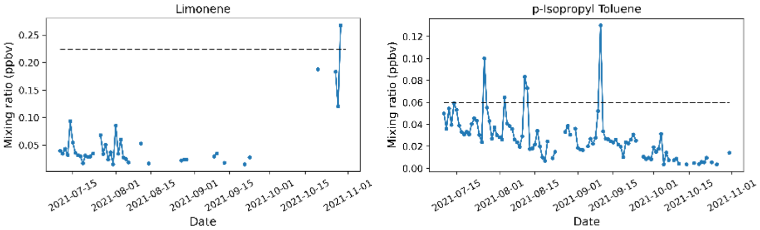

Figure 6-12: Time series of measured terpene concentrations.

6.8 Chamber Measurements

NO_x and O_3 concentrations were measured continuously inside the UCD mobile smog chambers during the entire study period. Here we report initial NO_x concentration, initial O_3 concentration and final O_3 concentration in the base-case chamber, together with measured O_3 sensitivity to NO_x and VOC perturbations ($\Delta O_3^{+NO_x}$ and ΔO_3^{+VOC}). The initial NO_x and O_3 concentration reflect daily ambient NO_x and O_3 concentration between 10 AM and 12 PM. The final O_3 concentration reflects the O_3 formed in the base-case chamber with constant UV intensity. Note that final chamber O_3 concentrations are frequently higher than ambient measurements because the latter are influenced by atmospheric mixing and dilution (Wu et al., 2022). Both the initial and final O_3 concentrations have a declining seasonal trend, especially after August.

$\Delta O_3^{+NO_x}$ in Figure 6-13 represents the difference between O_3 concentration measured in the NO_x perturbed chamber and the base-case chamber after the 3-hour UV exposure. ΔO_3^{+VOC} represents the difference between the O_3 concentration measured in the VOC perturbed chamber and the base-case chamber. A detailed description of the chamber measurement is discussed by Wu et al. (2022). A positive value of $\Delta O_3^{+NO_x}$ indicates that O_3 sensitivity is in the NO_x-limited regime, while a negative value of $\Delta O_3^{+NO_x}$ indicates the VOC-limited (NO_x-rich) regime. O_3 formation is generally NO_x-limited on weekends at the start of the experiment, but trends towards VOC-limited (NO_x-rich) at the end of the experiment. This pattern is generally consistent with previous measurements made in Sacramento (Wu et al., 2022).

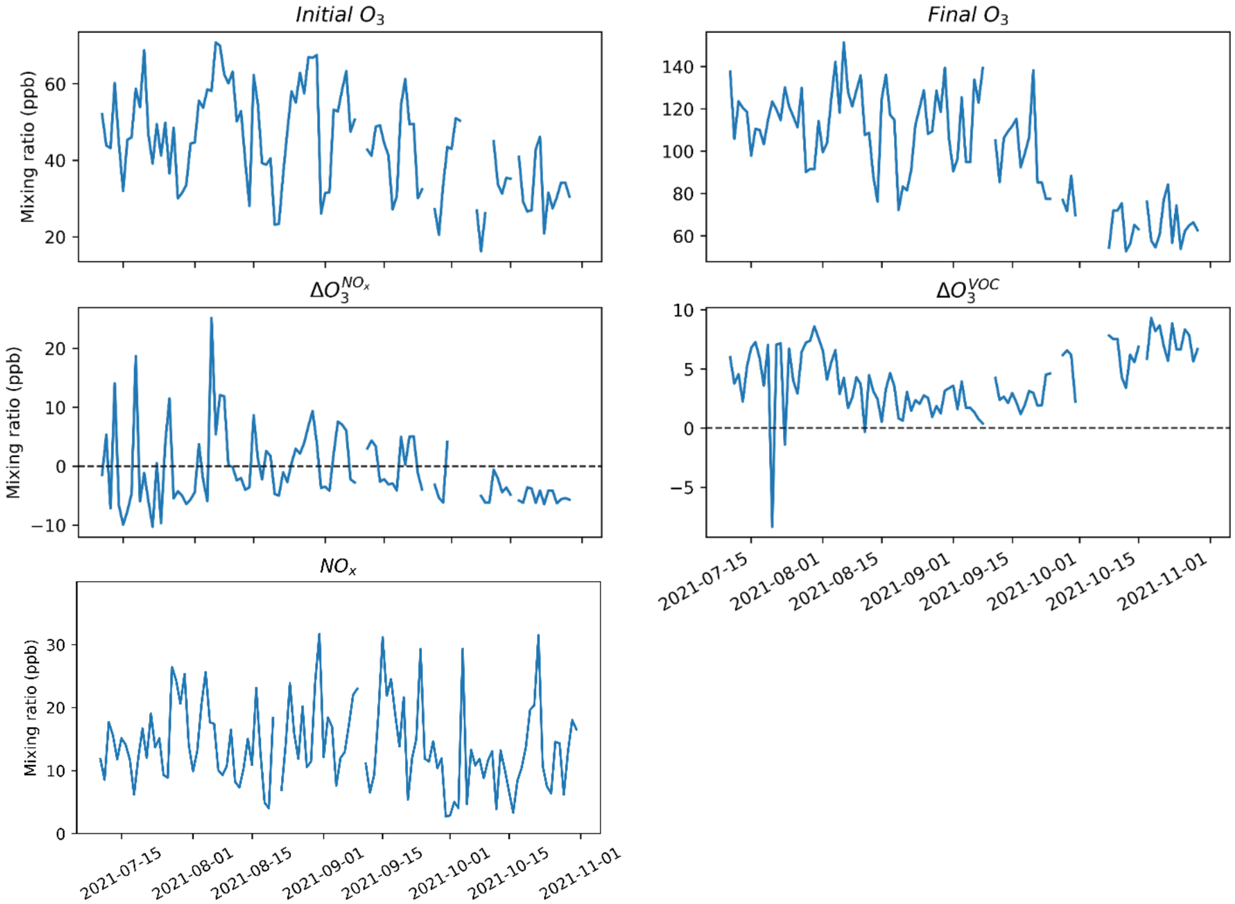

Figure 6-13: Time series of measured NO_x (in basecase chamber), O_3 concentrations (in basecase chamber, 'initial' = before UV lights on; 'final' = after 3hr UV exposure) and O_3 perturbation response. All measurements were made using UCD mobile smog chambers.

7 MEASUREMENT TRENDS ANALYSIS and DISCUSSION

7.1 Weekday & weekend difference

Weekday vs. weekend concentrations differences were analyzed for all measured compounds using a hypothesis test based on a null hypothesis of equal values during the two time periods. Lower p-values reject the null hypothesis in favor of an alternative hypothesis stating that concentrations on weekdays and weekends are different. Strong day of week patterns are expected for compounds emitted from traffic-related sources. A t-test for weekday and weekend ambient NO_x concentration showed a low P-value (<0.001) during the sampling period, strongly suggesting that weekend effects existed for diesel engines.

Table -1 lists all the measured compounds that have p-value less than 0.1. Among all listed compounds only acrolein has a negative t-score, which means weekend concentrations were higher than weekday concentrations. It should be noted that acrolein (Figure 7-1) only has a few values above detection limits, mainly in the last month of the study period. Acrolein is emitted from multiple combustion sources including vehicles, wood fires, cooking, and incense (Cahill, 2014). Several of these sources are typically more active on weekends (e.g., barbeque cooking). All other compounds in Table 7-1 have higher weekday concentrations than weekend concentrations.

Table 7-1 T-test results on weekday & weekend comparison (only compounds with p-value ≤ 0.2 are shown)

Parameter	T-score	p-value	Group
m,p-Tolualdehyde	3.185391	0.002079	Aldehyde
Parachlorobenzotrifluoride	2.37871	0.019234	Halogen
1-Methylnaphthalene	2.348084	0.022428	Alkene
2-Methylnaphthalene	2.228265	0.029077	Alkene
Benzene, propyl-	2.215267	0.029183	Aromatic
Acetaldehyde	2.197977	0.030546	Aldehyde
Ethane, 1,1,1,2-tetrachloro-	2.221797	0.032019	Halogen
Acrolein	-2.22081	0.038719	Aldehyde
o-Cresol	2.025277	0.047371	Hydroxyl
Naphthalene	1.865323	0.065802	Alkene
m,p-Xylene	1.803569	0.074251	Alkene
N-Nitrosodimethylamine	1.811992	0.074339	Amine
Dichloromethane	1.796421	0.075478	Halogen
o-Xylene	1.784813	0.077264	Alkene
p-Cresol	1.775797	0.079992	Hydroxyl
N-Butane	1.707215	0.091015	Alkane
Isobutane	1.676654	0.096864	Alkane

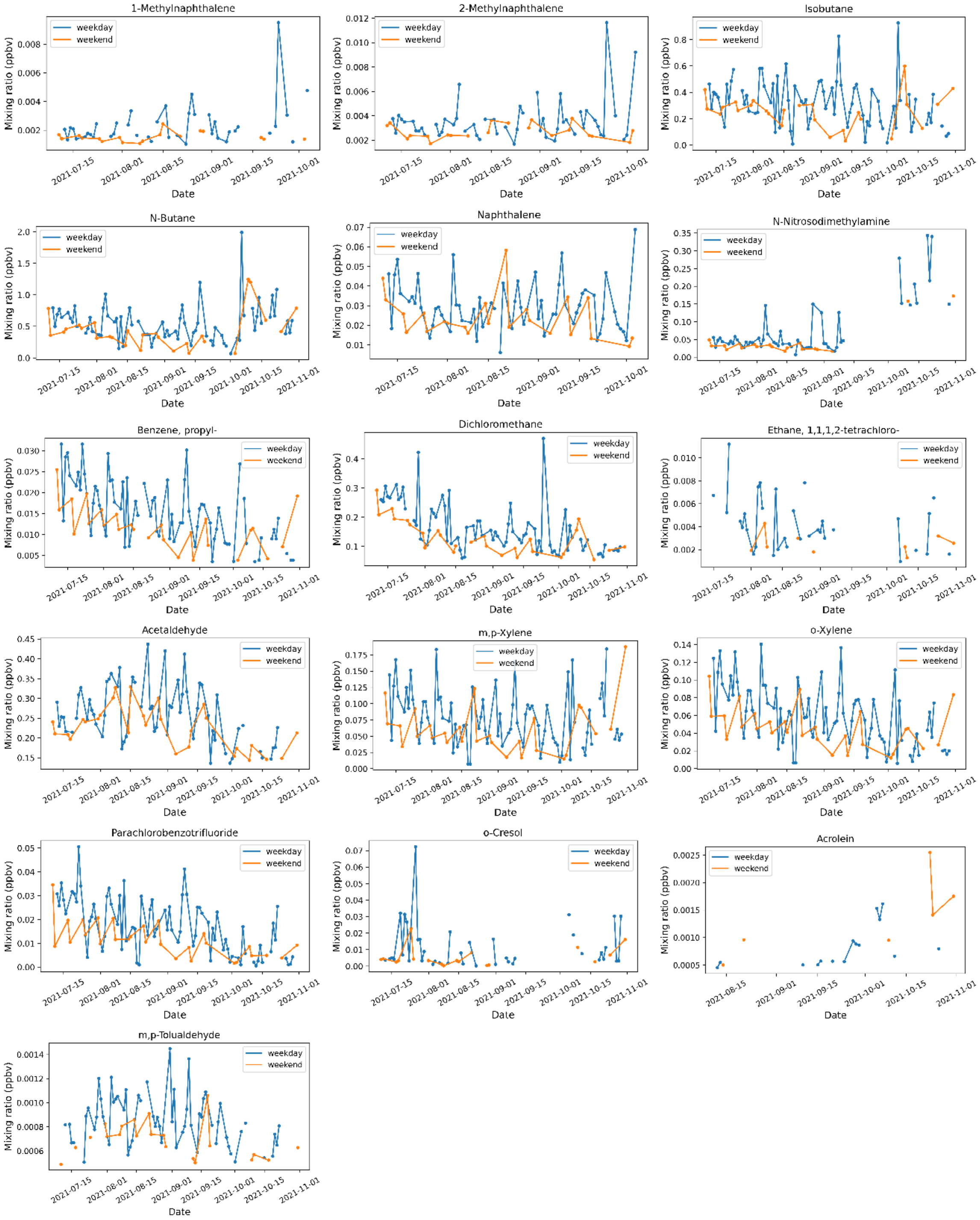
1-Methylnaphthalene
2-Methylnaphthalene
Isobutane
N-Butane
Naphthalene
N-Nitrosodimethylamine
Benzene, propyl-
Dichloromethane
Ethane, 1,1,1,2-tetrachloro-
Acetaldehyde
m,p-Xylene
o-Xylene
Parachlorobenzotrifluoride
o-Cresol
Acrolein
m,p-Tolualdehyde

Figure 7-1: Time series of weekend vs. weekday concentrations. Missing data was below detection limits or failed QA/QC checks.

Typical traffic patterns in Southern California have lower levels of diesel vehicles on weekends (leading to decreased NO_x concentrations) and a later time for the pulse of gasoline vehicles. Both of these factors contribute to lower concentrations of traffic-related pollutants on weekends. Xylene and butane are compounds emitted from traffic sources that follow this trend in the current study.

Several other VOCs generally recognized as industrial solvents also exhibited higher weekday concentrations than weekend concentrations at the Redlands measurement site. These compounds include dichloromethane and parachlorobenzotrifluoride. Dichloromethane is used as a solvent in several industries including pharmaceuticals, chemicals, food processing, metal cleaning, and paint removal. Dichloromethane is also used in several consumer products including paints, sealants, adhesives, hairspray, etc. Parachlorobenzotrifluoride is used as a solvent in paint and coating formulations and the printing industry. The higher weekday concentrations of these compounds strongly suggest that they are derived from industrial uses rather than consumer products.

7.2 Seasonal Changes

At the longest time scales, seasonal trends are apparent for BTEX compounds and terpenes, suggesting that hotter temperatures are associated with higher rates of gasoline evaporative emissions and higher rates of biogenic emissions. Figure 7-2 below display the predicted temperature dependence for evaporative emissions predicted by the EMFAC2014 model (California Air Resources Board, 2011) and the biogenic emissions predicted by the MEGAN model (Guenther, Monson, & Fall, 1991) for Riverside, CA. All emissions are compared to basecase emissions on August 01, 2010, as a reference point.

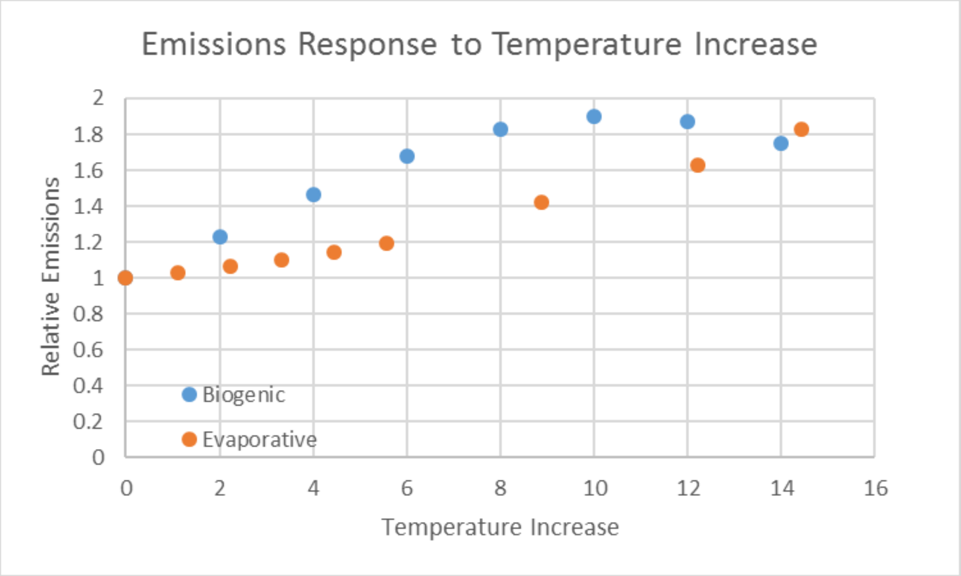

Figure 7-2: Effect of increasing temperature on biogenic emissions and mobile-source evaporative emissions.

Gasoline evaporative emissions occur during refueling, during normal operations (running), immediately after the vehicle turns off (hot soak), and while parked for extended periods (cold soak). Increasing temperatures increase gasoline evaporation rates from each one of these processes with little evidence of an upper threshold. In contrast, biogenic emissions initially increase with ambient temperature up to a peak of approximately 38^{o}C, followed by a slow decrease in emissions as temperatures increase beyond that level (Guenther et al., 2006). The results summarized in Figure *7-2* suggest that biogenic emissions respond more strongly to the increasing temperature at the Redlands site up to ΔT values greater than 10-15^{o}C, after which VOC evaporative emissions from motor vehicles respond more strongly.

Several VOCs display a time trend that increases from very low concentrations during the first half of the measurement period to significantly higher concentrations starting in September. This time period corresponds to the transition from summer blend gasoline to winter-blend gasoline, a shift in wind patterns, and the resumption of classes at nearby educational institutions. Compounds that follow this time pattern include acrolein (produced from heated cooking oil in cafeterias), D4 siloxane (used in insecticides and adhesives, as well as personal care products), nitrosodimethylamine (a research chemical), and 4-chloro-3-fluoro methyl phenol (preservative in paints and inks).

7.3 Histograms

Figures 7-3 through 7-14 display histograms of log-transformed daily concentration for each compound. Each histogram plot also displays a kernel density estimate (KDE) in red to visualize the theoretical distribution of concentrations as continuous probability density curves. Most compounds follow a log-normal shape with a few exceptions of bimodal behavior that may reflect different emissions sources or atmospheric production pathways. Concentration histograms are slightly truncated at lower levels for several compounds (heptane, n-hexane, trimethylbenzene), which may reflect the lower limits of detection. Concentration histograms are also slightly truncated at higher levels for several compounds (isopentane, ethylbenzene, toluene), which may reflect the saturation of the sample collection tubes.

Histograms of D5 siloxane concentrations followed a log-normal distribution typical of atmospheric concentrations influenced by turbulent fluctuations. In contrast, measured methanol concentrations peaked more than three times the standard deviation above median concentrations during several events. A possible methanol source is the decomposition of plant material, such as during composting (episodically released during turning), following lawn mowing, or other landscaping activities. Siloxanes and alcohols have been identified as markers for VCPs.

Halocarbon and Ketones

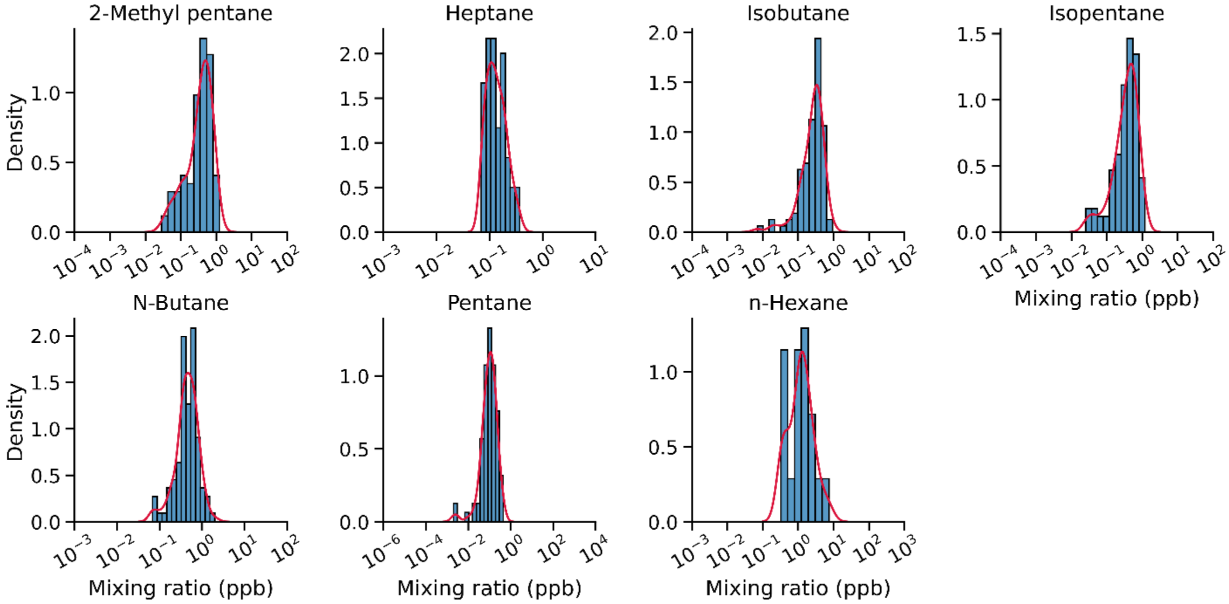

Figure 7-3: Histograms of measured alkane concentrations.

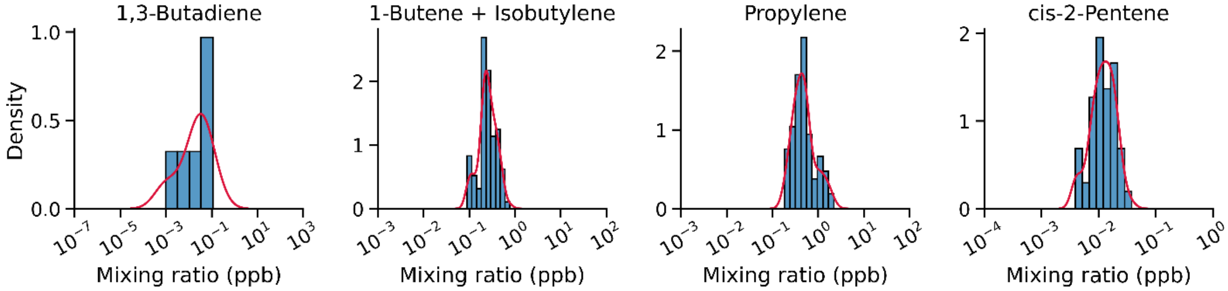

Figure 7-4: Histograms of measured alkene concentrations.

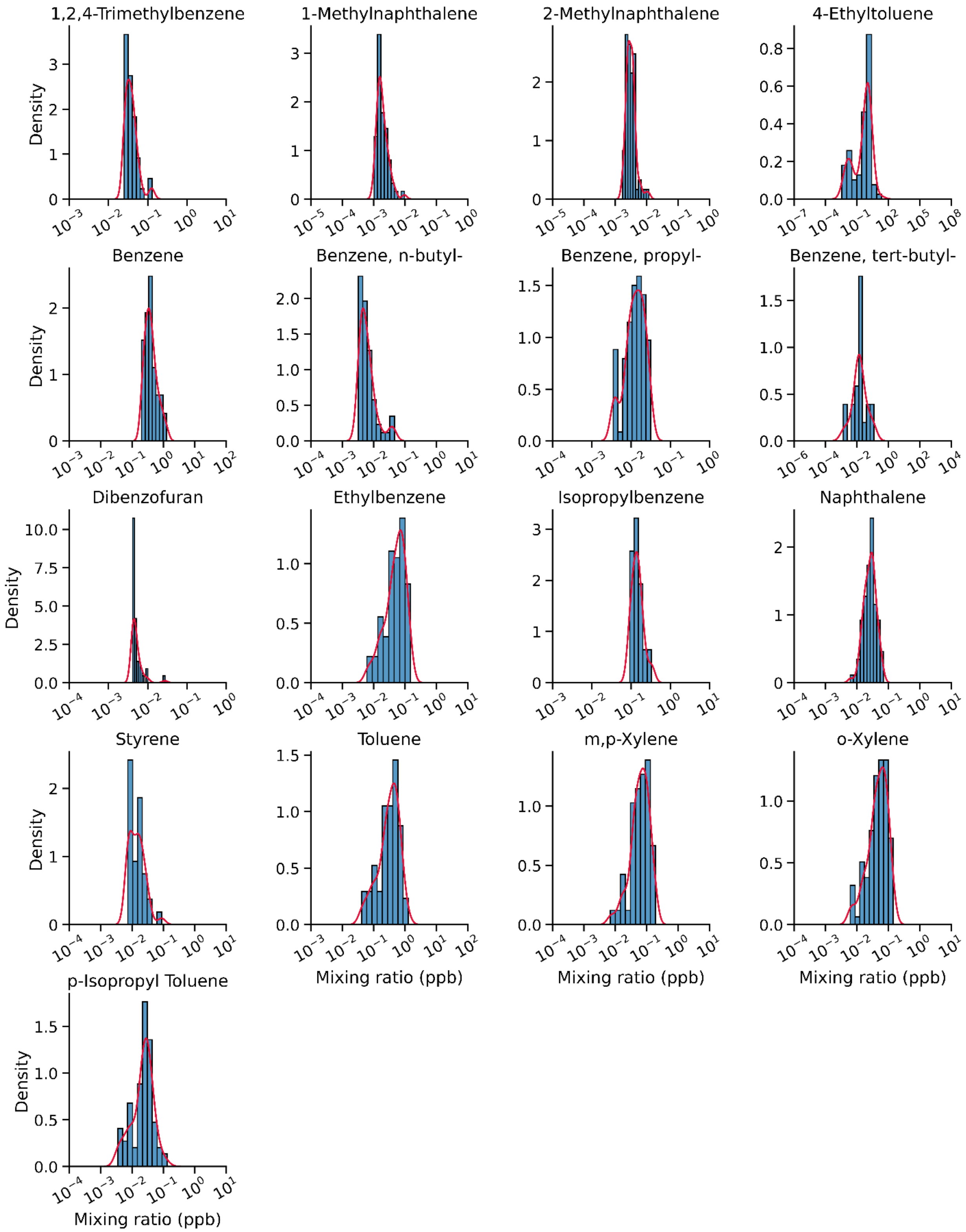

Figure 7-5: Histograms of measured aromatic concentrations.

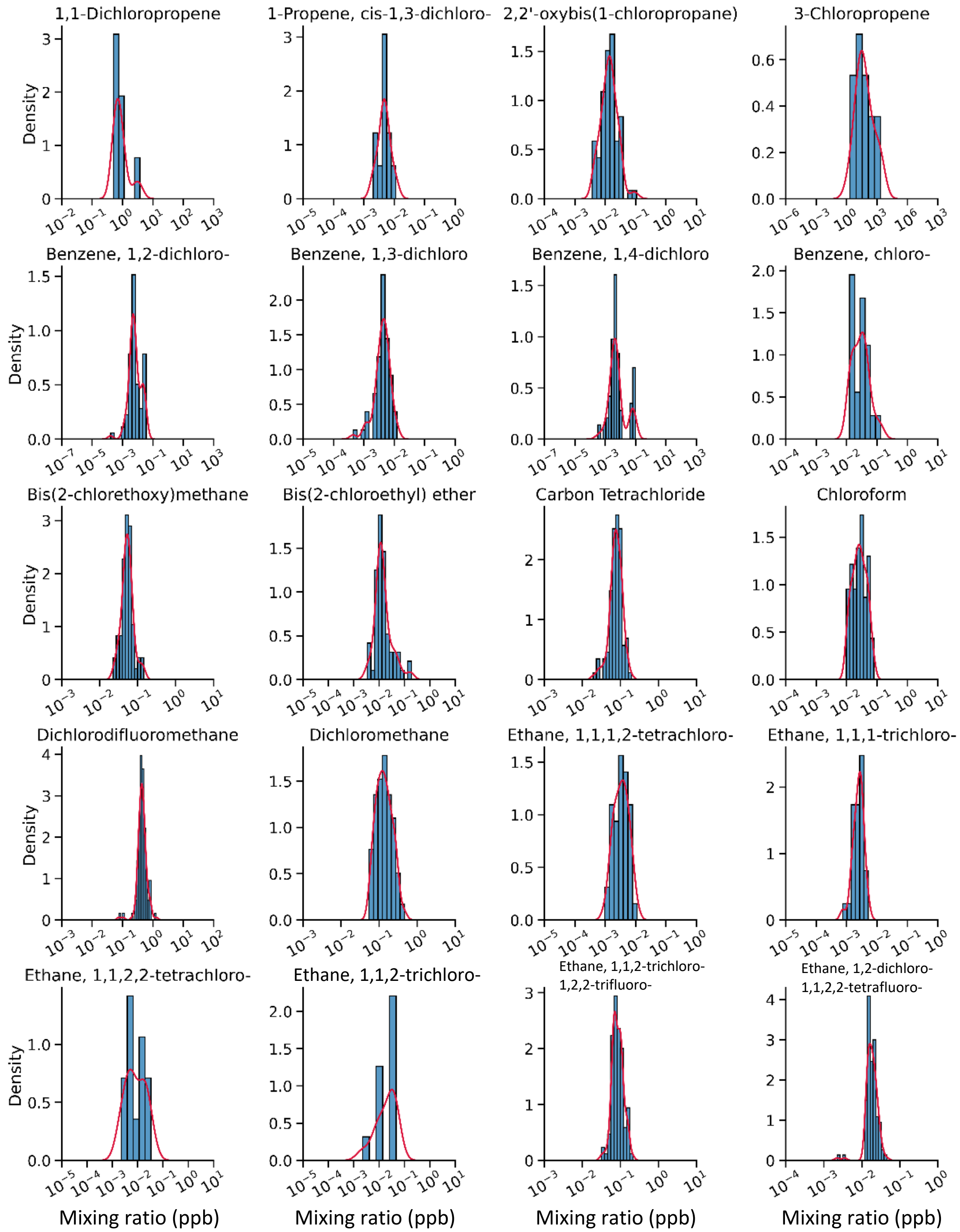

Continue to next page

Continue From last page

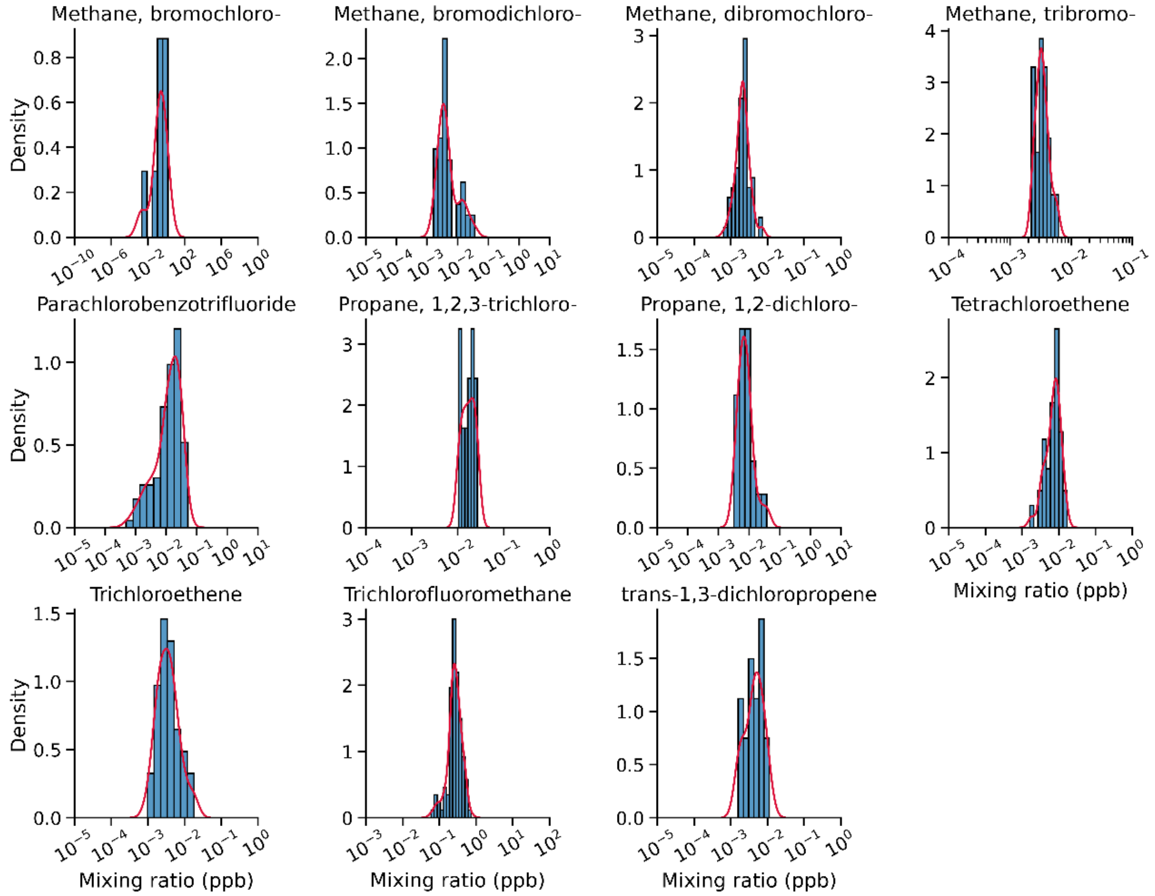

Figure 7-6: Histograms of measured halogenated concentrations.

Aldehydes and Ketones

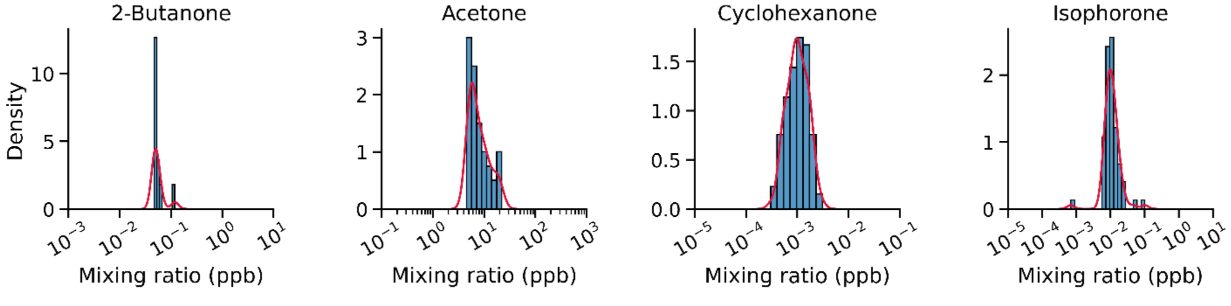

Figure 7-7:Time series of measured ketone concentrations.

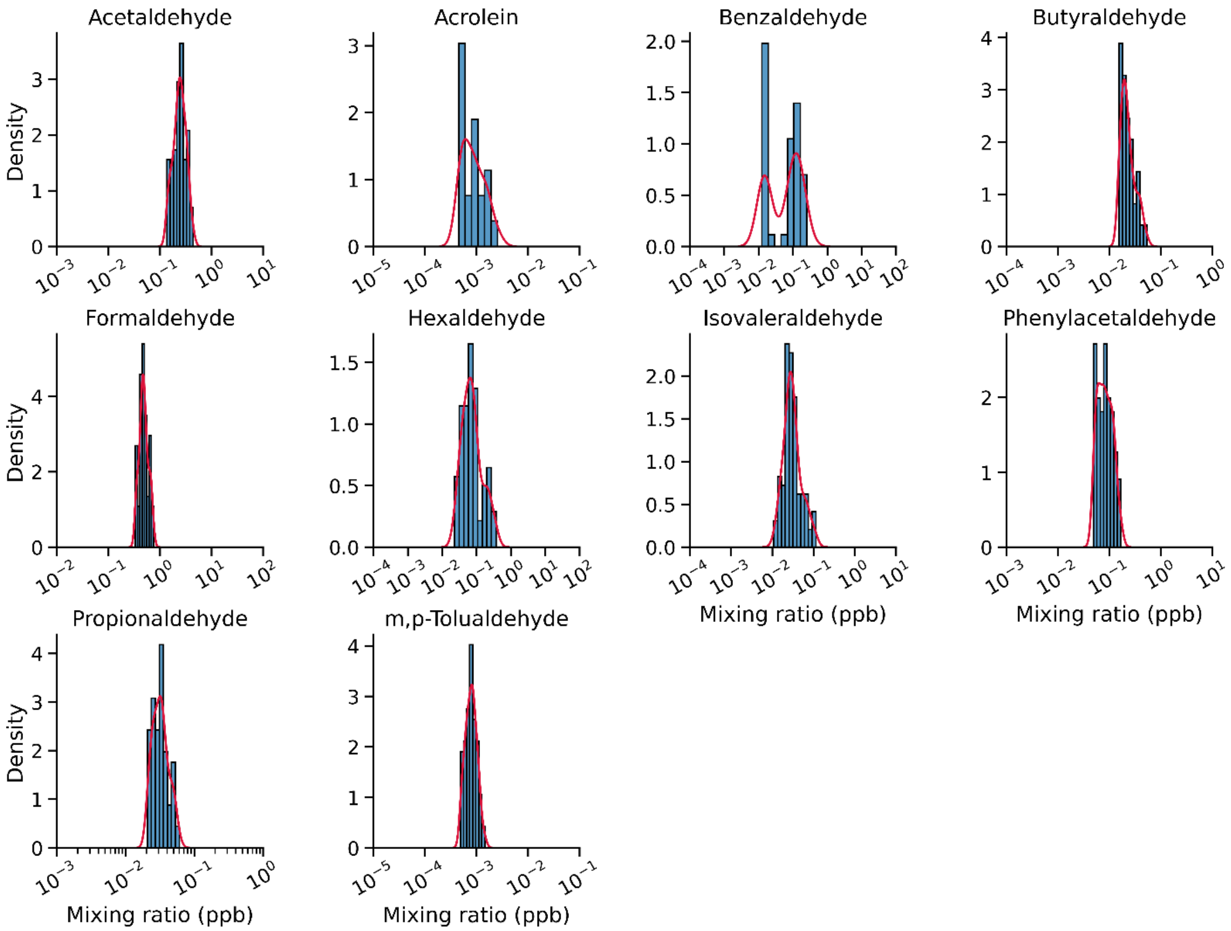

Figure 7-8: Histograms of measured aldehyde concentrations.

Alcohols and Phenolic Compounds

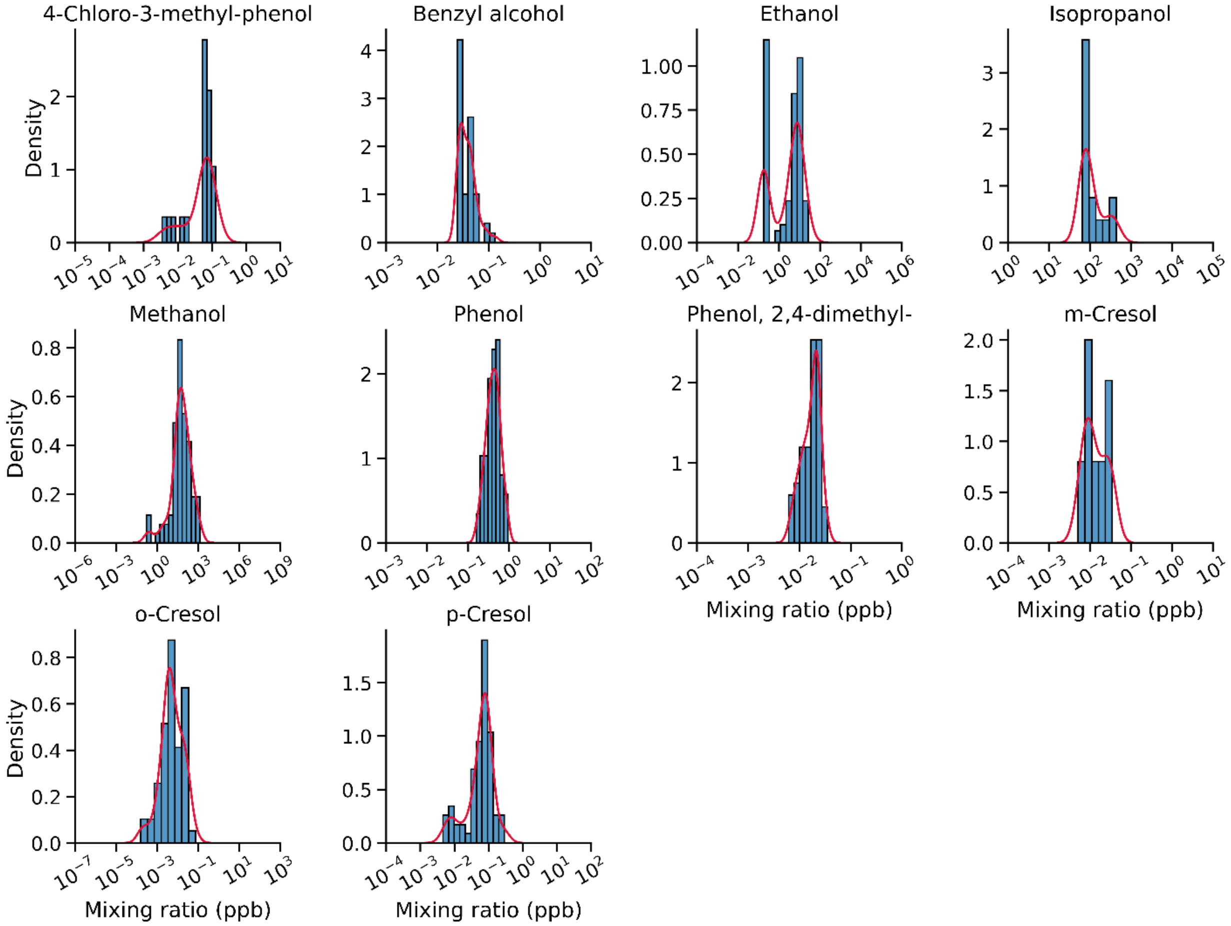

Figure 7-9: Histograms of measured alcohol and phenol concentrations.

Semi-volatile Organic Compounds

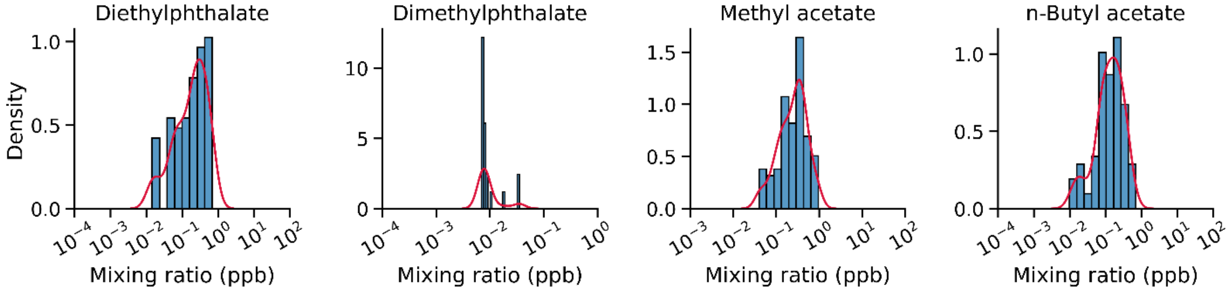

Figure 7-10: Histograms of measured ester concentrations.

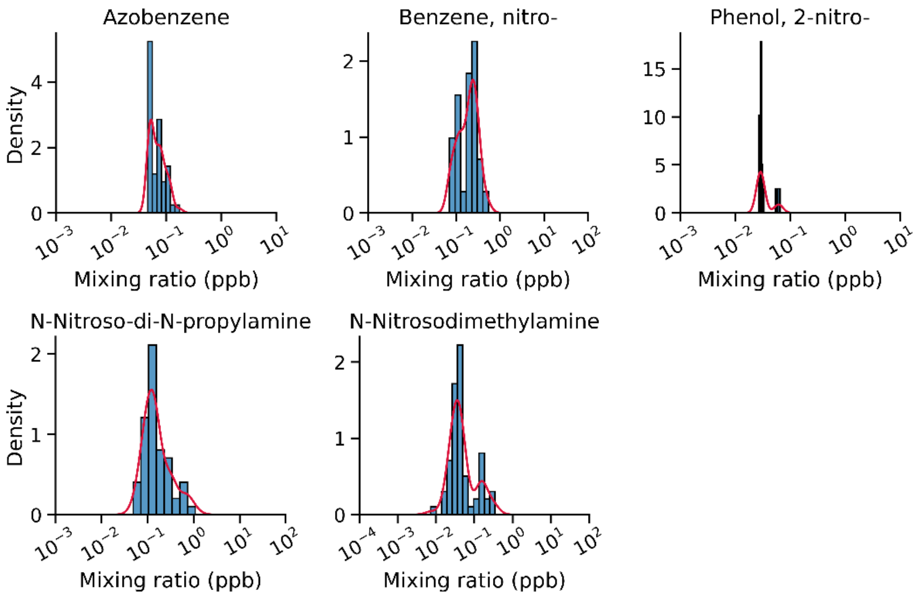

Figure 7-11*: Histograms of measured nitrogen-containing VOC concentrations*

Total Organic Silicon

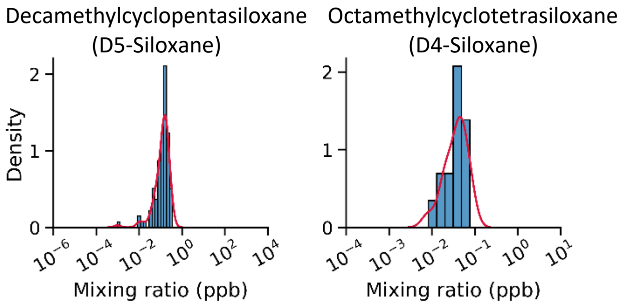

Figure 7-12: Histograms of measured siloxanes concentrations.

Terpenes

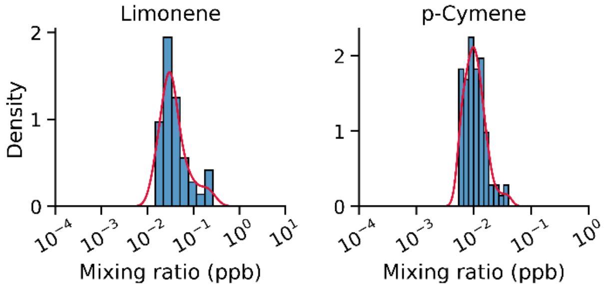

Figure 7-13: Histograms of measured terpenes concentrations.

Chamber Measurements

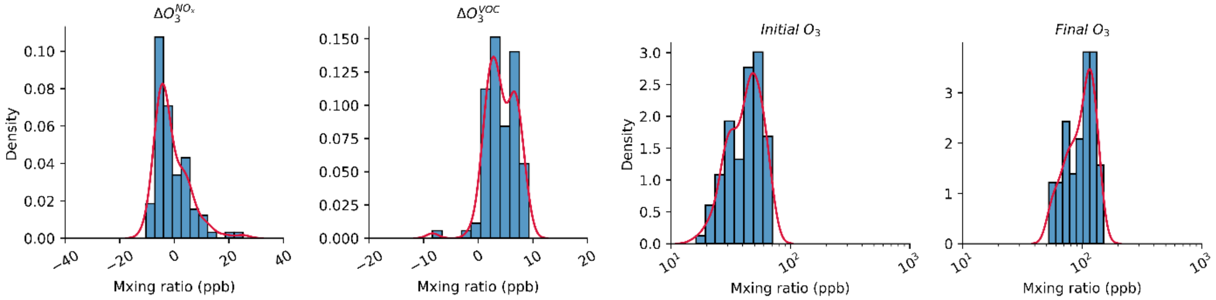

Figure 7-14: Histograms of measured O_3 concentrations and O_3 perturbation response.

7.4 Correlation analysis

Figure 7-15 illustrates the correlation matrix that compares relationships between different compound concentrations. Only compounds that have at least one correlation coefficient larger than 0.5 are shown in the correlation matrix. The color in each box in Figure 7-15 shows the correlation coefficient for a pair of compounds. A pair of compounds with the p-value > 0.05 are shown as a blank box, as their correlation is not significant. Final chamber O_3 formation (labeled as bag2_3hr) is positively associated with temperature and concentrations of various oxygenated compounds. This latter association likely reflects the fact that higher oxidant concentrations that produce O_3 also produce higher concentrations of oxygenated compounds. Final chamber O_3 concentrations have a strong negative association with compounds that peak in the fall months.

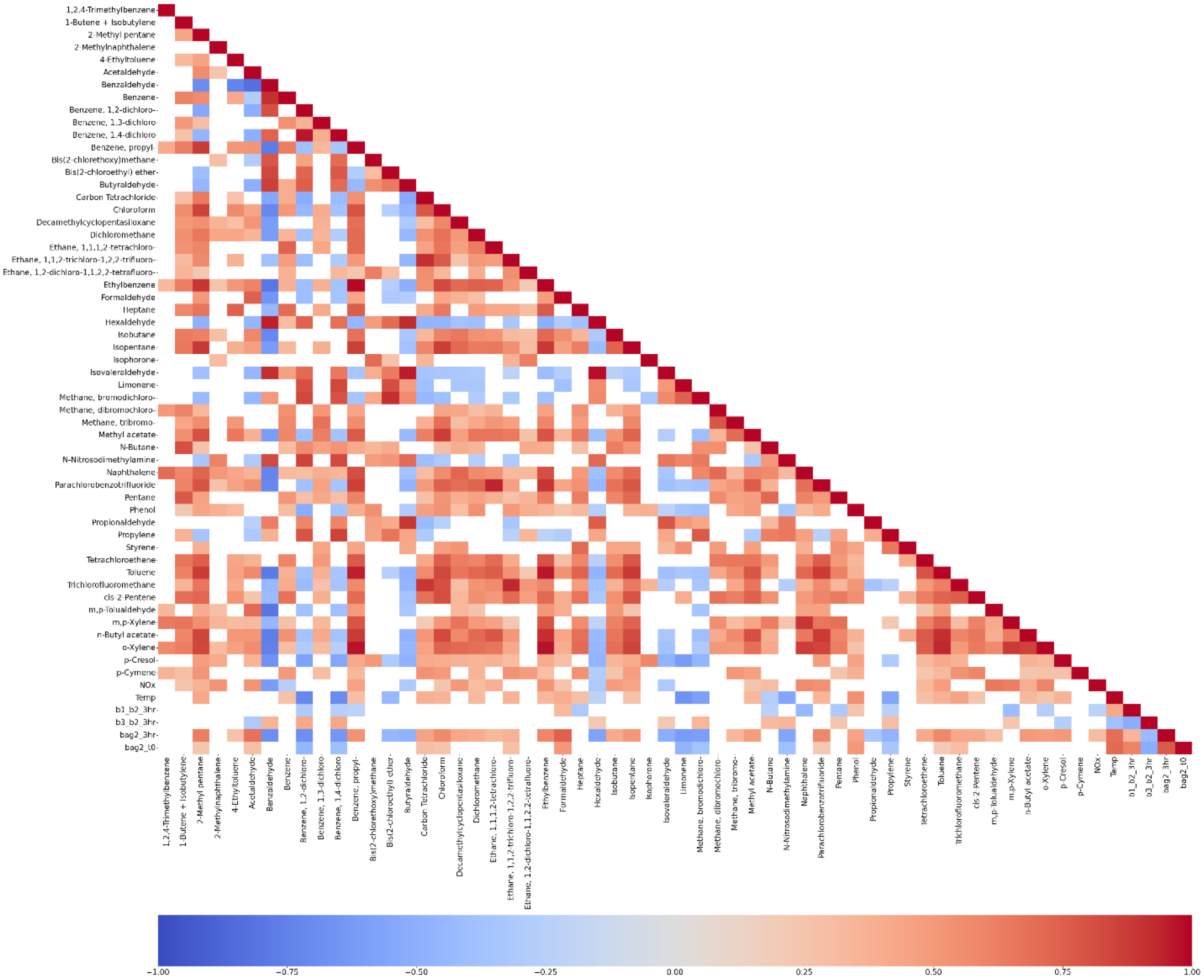

Figure 7-15: Correlation matrix between measured compounds and meteorological parameters. Blue color indicates a negative correlation, red color indicates a positive correlation, and blank indicates no correlation.

7.5 Comparison with previous studies

Table 7-2 compares the VOC concentrations measured in the current study with previous VOC measurements in the SoCAB as a QA/QC exercise. The first comparison dataset was obtained from the Photochemical Assessment Monitoring Stations (PAMS) network. The Riverside PAMS site is located approximately 26 km southwest of the Redlands monitoring site. PAMS data is reported with hourly time resolution from June to September each year. PAMS measurements are available for the years 2019 and 2020, but not 2021, at the time of this analysis. Average PAMS concentrations measured between 10 am to 12 pm in the years 2019-2020 were compared to measurements made over the same hours in 2021 in the current study. Concentrations of larger alkanes and BTEX were higher at Riverside in the years 2019-2020 than at Redlands in 2021. Alkanes and BTEX compounds are generally related to oil and gas refining and traffic emissions (Brown et al., 2007). Riverside has a population more than four times larger than Redlands, and the PAMS site in Riverside is twice as close to a major freeway (750 m to I-60) than the measurement site in Redlands (1,500 m to I-10). The Riverside PAMS site is also located approximately 8 km to the southwest of the Bloomington fuel storage depot whereas the Redlands site is approximately 20 km to the northeast of the depot. Each of these factors could contribute to higher concentrations of fuel / traffic-related emissions at the Riverside monitoring site. Other chemicals (e.g., alkenes and aromatic compounds) were measured at similar concentrations at Riverside and Redlands.

Van Rooy et al. (2021) measured VOC concentrations at Irvine and Riverside, CA, from April to July 2020 to characterize changes to VOC concentrations under COVID-19 lockdown conditions. The SoCAB-2020 data shown in the final column of Table 8-1 was collected in the morning between 9 AM and 10 AM PDT. Several species that were missing in the morning period were measured in the afternoon between 2 PM and 3 PM PDT. Concentrations of alkanes, aromatic, and halogenated compounds are similar in the SoCAB-2020 and Redlands-2021 datasets. Concentrations of some alkenes (e.g., propylene, butene, etc.) and BTEX compounds in SoCAB-2020 were slightly lower than corresponding concentrations in the Redlands-2021 dataset. The lower concentrations of compounds related to on-road emissions may reflect the effects of reduced travel during COVID-19 shutdown periods (Chossière et al., 2021; Cooper et al., 2022; Liu et al., 2020). Limonene and some oxygenated compounds (e.g., Benzaldehyde, methyl acetate) were present at lower concentrations in the SoCAB-2020 dataset. Limonene is a biogenic VOC with an emissions rate that depends on temperature and light. Oxygenated compounds are most likely secondary products with a formation rate that also depends on temperature and light intensity. The sampling period for the SoCAB-2020 study was mainly in the Spring, while the sampling period for the Redlands-2021 study was mainly in the Summer and early Fall. These factors may explain the difference between the concentrations measured during the separate campaigns.

Table 7-2 Comparison of measured VOC concentrations with previous studies in the SoCAB

Parameter	**Redlands-2021**			**PAMS-2019**	**PAMS-2020**	**SoCal-2020**
	mean (ppb)	**min (ppb)**	**max (ppb)**	**mean (ppb)**	**mean (ppb)**	**mean (ppb)**
Alkane						
n-Butane	0.5144	0.0680	1.9883	1.8523	2.7232	0.7000
Isobutane	0.3011	0.0070	0.9255	1.0662	1.2030	0.3400
n-Pentane	0.1232	0.0020	0.4355	1.6932	1.7626	0.2530
Isopentane	0.4244	0.0250	1.1805	3.9884	4.3897	0.5490
n-Hexane	1.5926	0.3235	7.3494	0.7668	0.8304	0.1210
Heptane	0.1459	0.0698	0.3709			0.0440
2-Methyl pentane (Isohexane)	0.4272	0.0284	1.2301			0.1330
Alkene						
Propylene	0.5753	0.1820	2.1985	0.3847	0.5836	0.1390
1-Butene + Isobutylene	0.2733	0.0890	0.7680	0.1544	0.2261	0.0860
cis-2-Pentene	0.0133	0.0039	0.0378			0.0040
1,3-Butadiene	0.0364	0.0010	0.1113			0.0140
Terpene						
Limonene	0.0507	0.0147	0.2677			0.005*

Parameter	Redlands-2021			PAMS-2019	PAMS-2020	SoCal-2020
p-Cymene	0.0115	0.0054	0.0403			
Aromatic						
Benzene	0.4458	0.2019	1.2587	0.8234	0.8256	0.1410
Toluene	0.3811	0.0413	1.2599	1.9425	1.9656	0.2850
Ethylbenzene	0.0595	0.0061	0.1491	0.3398	0.3395	0.0360
m,p-Xylene	0.0733	0.0069	0.1875	0.6982	0.7191	0.1130
o-Xylene	0.0556	0.0061	0.1405	0.3205	0.3502	0.0450
Styrene	0.0172	0.0074	0.0874	0.0207	0.0132	0.0110
Isopropylbenzene	0.1536	0.0923	0.3315			0.0040
Benzene, propyl-	0.0144	0.0035	0.0316			0.0080
Benzene, n-butyl-	0.0082	0.0032	0.0457			
Benzene, tert-butyl-	0.0247	0.0013	0.1195			
p-Isopropyl Toluene	0.0280	0.0035	0.1301			
1,2,4-Trimethylbenzene	0.0415	0.0253	0.1299	0.1744	0.2053	0.0300
4-Ethyltoluene	1.1058	0.0035	21.7571	0.7848	0.4335	0.0120
Naphthalene	0.0282	0.0061	0.0689			
2-Methylnaphthalene	0.0033	0.0017	0.0116			
1-Methylnaphthalene	0.0021	0.0010	0.0095			
Siloxane						
D4-Siloxane	0.0412	0.0083	0.0766			
D5-Siloxane	0.1435	0.0010	0.3536			
Halogenated						
Chloroform	0.0301	0.0098	0.0786			0.0340
Carbon Tetrachloride	0.0815	0.0193	0.1966			0.0790
Dichloromethane	0.1531	0.0544	0.4698			0.0560
Methane, bromochloro-	0.0143	0.0003	0.0426			
Methane, dibromochloro-	0.0023	0.0006	0.0073			0.0040
Methane, bromodichloro-	0.0068	0.0016	0.0358			
Methane, tribromo-	0.0035	0.0022	0.0063			0.0050
Dichlorodifluoromethane	0.4617	0.0756	1.2992			
Trichlorofluoromethane	0.2854	0.0592	0.7353			
Ethane, 1,1,1-trichloro-	0.0026	0.0007	0.0051			
Ethane, 1,1,2-trichloro-	0.0250	0.0022	0.0470			
Ethane, 1,1,1,2-tetrachloro-	0.0039	0.0010	0.0112			
Ethane, 1,1,2,2-tetrachloro-	0.0116	0.0022	0.0336			
Ethane, 1,2-dichloro-1,1,2,2-tetrafluoro-	0.0192	0.0022	0.0454			
Ethane, 1,1,2-trichloro-1,2,2-trifluoro-	0.0898	0.0314	0.2134			
Trichloroethene	0.0045	0.0010	0.0179			
Tetrachloroethene	0.0076	0.0016	0.0167			
3-Chloropropene	3.7018	0.1665	17.0992			

Parameter		**Redlands-2021**		**PAMS-2019**	**PAMS-2020**	**SoCal-2020**
Propane, 1,2,3-trichloro-	0.0179	0.0105	0.0269			
Propane, 1,2-dichloro-	0.0093	0.0032	0.0381			
1,1-Dichloropropene	1.0663	0.5075	3.7117			
trans-1,3-dichloropropene	0.0050	0.0016	0.0112			
1-Propene, cis-1,3-dichloro-	0.0052	0.0020	0.0112			
Benzene, chloro-	0.0358	0.0125	0.1322			
Benzene, 1,2-dichloro-	0.0097	0.0002	0.0361			
Benzene, 1,3-dichloro	0.0047	0.0004	0.0122			
Benzene, 1,4-dichloro	0.0156	0.0003	0.0972			0.001*
4-Chloro-3-methyl-phenol	0.0599	0.0035	0.1287			
Bis(2-chlorethoxy) methane	0.0572	0.0225	0.1441			
Bis(2-chloroethyl) ether	0.0217	0.0034	0.1890			
2,2'-oxybis(1-chloropropane)	0.0169	0.0037	0.1073			
Parachlorobenzotrifluoride	0.0156	0.0005	0.0505			
		<u>Oxygenated</u>				
Methanol	144.7257	0.1590	1307.2416			
Ethanol	104.8955	18.2605	769.0682			
Isopropanol	142.9751	64.7270	445.9840			
Phenol	0.4366	0.1573	0.9243			
Phenol, 2,4-dimethyl-	0.0178	0.0061	0.0351			
Benzyl alcohol	0.0412	0.0243	0.1337			
p-Cresol	0.0748	0.0046	0.2866			
m-Cresol	0.0164	0.0052	0.0351			
o-Cresol	0.0098	0.0002	0.0723			
2-Butanone	0.1359	0.1119	0.2823			0.064*
Isophorone	0.0309	0.0017	0.2416			
Cyclohexanone	0.0026	0.0007	0.0074			0.01*
Acetone	20.875	10.806	52.018	16.053	18.476	
Acrolein	0.0024	0.0010	0.0060	0.966	0.628	
Propionaldehyde	0.0781	0.0000	0.1441			
Isovaleraldehyde	0.0829	0.0257	0.2721			
Benzaldehyde	0.2031	0.0295	0.5972			0.006*
Formaldehyde	1.1753	0.7881	1.7791	4.020	5.130	
Butyraldehyde	0.0576	0.0364	0.1271			
Acetaldehyde	0.5919	0.3241	1.0410	3.437	5.132	
m,p-Tolualdehyde	0.0019	0.0012	0.0033			
Phenylacetaldehyde	0.2060	0.1167	0.3917			
Hexaldehyde	0.2264	0.0548	0.8814			
n-Butyl acetate	0.1737	0.0098	0.6951			
Diethyl phthalate	0.2517	0.0144	0.6885			

Parameter	Redlands-2021			PAMS-2019	PAMS-2020	SoCal-2020
Dimethyl phthalate	0.0109	0.0070	0.0352			
Methyl acetate	0.3059	0.0399	0.9520			0.006*
Dibenzofuran	0.0056	0.0041	0.0274			
		Other				
Azobenzene	0.0725	0.0460	0.1737			
Benzene, nitro-	0.2050	0.0706	0.5428			
Phenol, 2-nitro-	0.0349	0.0270	0.0667			
N-Nitroso-di-N-propylamine	0.2096	0.0485	1.0856			
N-Nitrosodimethylamine	0.0689	0.0073	0.3436			

* Indicates concentration measured at afternoon (2~3PM) in SoCAB.

8 PMF ANALYSIS

8.1 PMF model setup

A total of 32 VOC species were used as inputs for the PMF analysis (Table 8-1). Each of these input VOC species was recognized as a characteristic marker emitted by a limited number of primary pollutant sources (e.g., Siloxane for VCP sources and Terpenes for Biogenic sources) and they were measured above detection limits in a sufficient number of samples to support the PMF analysis (n≥60). The LOD of each VOC species is listed in Section 4.3.

Table 8-1 List of VOC species used as inputs for PMF calculation (grouped by functionality)

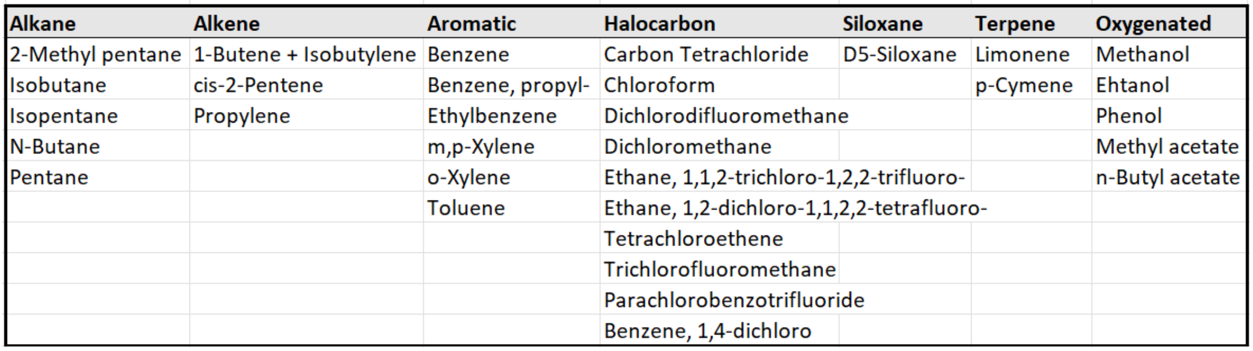

Alkane	Alkene	Aromatic	Halocarbon	Siloxane	Terpene	Oxygenated
2-Methyl pentane	1-Butene + Isobutylene	Benzene	Carbon Tetrachloride	D5-Siloxane	Limonene	Methanol
Isobutane	cis-2-Pentene	Benzene, propyl-	Chloroform		p-Cymene	Ehtanol
Isopentane	Propylene	Ethylbenzene	Dichlorodifluoromethane			Phenol
N-Butane		m,p-Xylene	Dichloromethane			Methyl acetate
Pentane		o-Xylene	Ethane, 1,1,2-trichloro-1,2,2-trifluoro-			n-Butyl acetate
		Toluene	Ethane, 1,2-dichloro-1,1,2,2-tetrafluoro-			
			Tetrachloroethene			
			Trichlorofluoromethane			
			Parachlorobenzotrifluoride			
			Benzene, 1,4-dichloro			

O_3 formation over the 3 hr base-case chamber experiment was also used as an input to the PMF analysis to identify associations between high O_3 concentrations and VOC sources. The O_3 formation in the base-case chamber was calculated as the final 3-hour O_3 concentration minus the initial O_3 concentration. The LOD for O_3 formation was set at 2 ppb based on blank tests that filled each chamber with zero air (Wu et al., 2022). All chambers (including the base-case) employed constant UV lights, and so the O_3 formation is mainly controlled by the VOC and NO_x concentrations in the ambient air, with lesser influence from meteorological conditions such as temperature and relative humidity (RH). It should be noted that O_3 formation is non-linear and many of the parent VOCs that generated O_3 may have undergone chemical reactions before the air mass reached the measurement site. Therefore, changes to O_3 formation may not be directly caused by changes in the measured VOC concentrations. Nevertheless, the incorporation of the O_3 formation into the PMF analysis will yield information that can help understand associations between high O_3 concentrations and sources.

PMF requires uncertainty estimates for all input species. The analytical uncertainty (μ_{ij}) for VOC species detected through GC-MS was determined to be 5%, and μ_{ij} for VOC species detected through LC-MS was determined to be 10% based on replicate analyses of target compounds in analytical standards and associated quality control samples. The analytical uncertainty for O_3 formation was set as 2.83%, which combines the analytical uncertainty of the O_3 monitor (2%) (2B Technologies, 2018) and the uncertainty of the chamber measurement (2%) (Wu et al., 2022).

PMF analysis was carried out using EPA PMF v5.0. A detailed description of the EPA PMF v5.0 software can be found in (U.S. Environmental Protection Agency, 2014). The PMF software calculates a signal-to-noise (S/N) ratio for the input data based on the measured concentrations and estimated uncertainty. Species with S/N value > 1 were defined as "Strong" species. Species with S/N between 0.5 to 1 were defined as "weak" species. Almost all the input species had S/N values > 1 in the current study ("Strong" species). Limonene had S/N = 3.4 but limonene concentrations above LOD were only available for approximately 1/3 of the total sampling days. Limonene was therefore categorized as a "Weak" species with uncertainty inflated by a factor of three.

The PMF solution with the minimum Q-score was generated using 100 base model runs initiated with different random seeds. The stability of the factors within the optimal Q-score solution was evaluated using 100 bootstrap runs. Multiple sets of analyses were conducted using different numbers of factors. The optimal number of factors in the final solution was determined by several criteria: 1) relatively low Q scores; 2) stable solution across 80% of bootstrap runs 3) small values for base model displacement (DISP) analysis; and 4) reasonable factor profiles based on known emissions composition.

PMF calculations were carried out with and without O_3 formation as an input species to ensure that the addition of O_3 formation did not substantially alter the VOC factor profiles. Careful analysis of the PMF results led to the selection of an eight-factor solution when not using O_3 formation as an input species (see SI). Adding O_3 formation to the input species did not significantly change the factor composition profiles or the factor concentration time series. The O_3 formation can be separated into different factors without changing the VOC factor apportionment results.

PMF results were post-processed to calculate conditional probability functions (CPFs) that identify the upwind direction of PMF-resolved factors. The CPF calculation combines the time series of PMF factor concentrations with wind direction data as described by Equation (8):

$$CPF = \frac{m_{\Delta\theta}}{n_{\Delta\theta}} \tag{8}$$

where $m_{\Delta\theta}$ is the number of occurrences when factor concentrations exceed a threshold value and wind comes from direction $\Delta\theta$, while $n_{\Delta\theta}$ is the total number of data points with wind direction

$\Delta\theta$. Threshold values equal to 25% of average concentrations were used in the current study, while $\Delta\theta$ was set as 22.5°.

Past studies (Kim et al., 2004; Xie and Berkowitz, 2006) have used CPF scores to analyze the source impact from various wind directions. In the current study, wind speed and wind direction measurements were obtained from the monitoring station adjacent to the measurement trailer. Only measurements between 10 AM and 12 PM were used in the analysis, corresponding to the chamber fill times. Wind roses of CPF scores are plotted to help understand the directionality of each PMF-resolved factor.

8.2 PMF analysis results

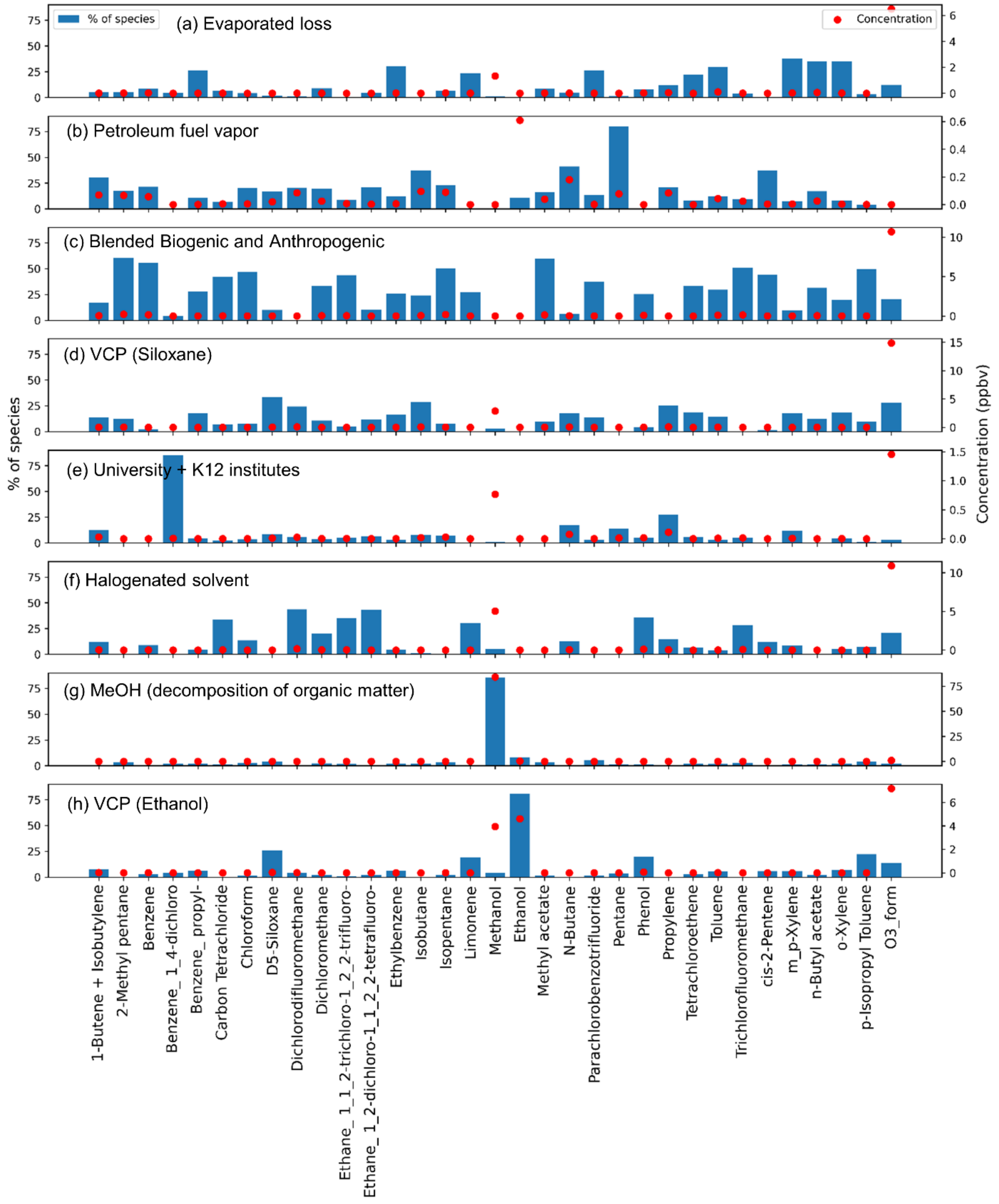

Figure 8-1 PMF factors and assigned source names : (a) liquid fuel evaporation, b) petroleum fuel vapor, c) biogenic, d) VCP (Siloxane), e) university and K-12 institutions, f) halogenated solvent, g) MeOH (decomposition of organic matter), and h) VCP (Ethanol). Input species listed on the x-axis. The blue bar (left y-axis) indicates the percentage (%) of a species apportioned to a source factor. The red dot (right y-axis) indicates the concentration (ppbv) of a species in a source factor.

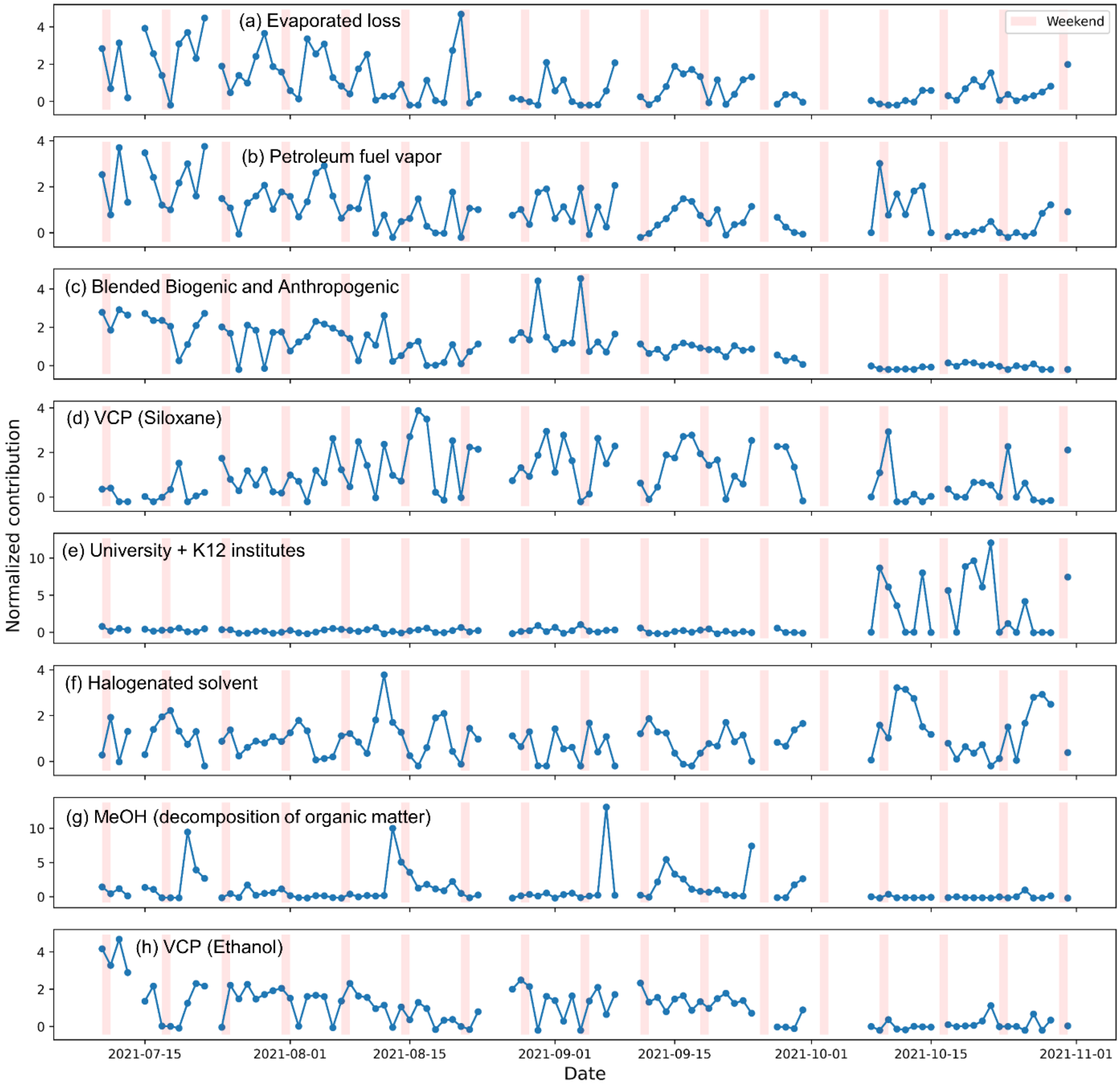

Figure 8-2 Time series of factor normalized contributions. The order of every source factor is consistent with factor profile (Figure 8-1). The y axis displays the normalized contribution in which the sum of factor concentrations equals 1. The shaded areas correspond to weekends.

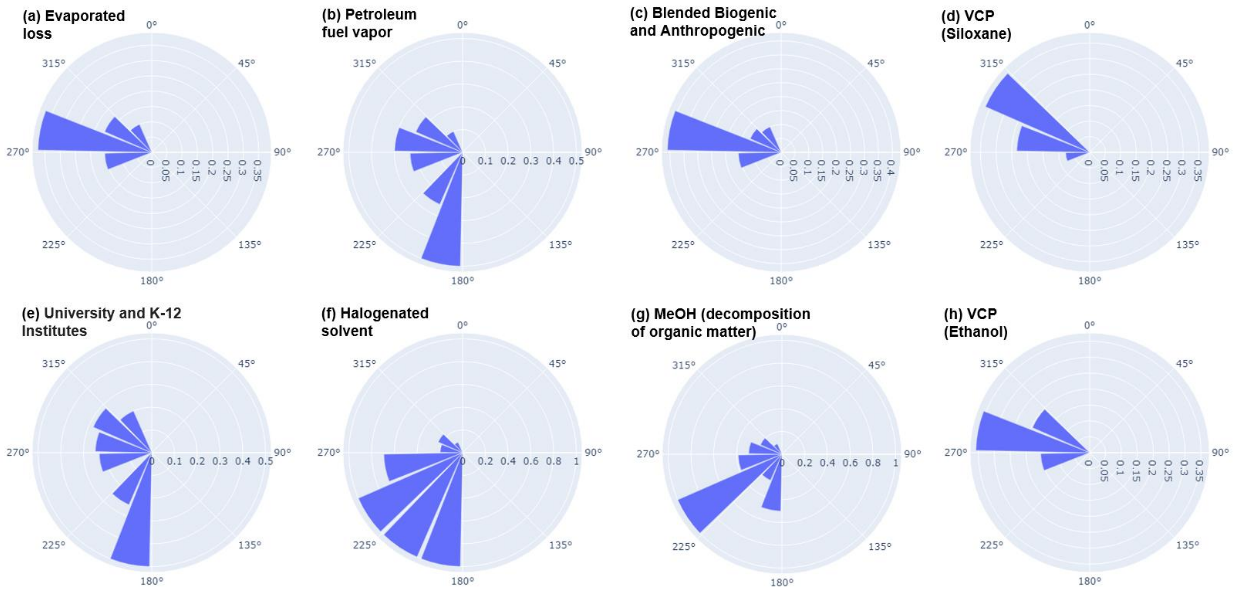

Figure 8-3 Wind rose of conditional probability function (CPF) for the highest 25% of the mass contribution from PMF-resolved factors.

8.2.1 Factor 1: Evaporation loss

Factor 1 contains a large fraction (> 30%) of three “BTEX” compounds Toluene, Ethylbenzene, and Xylene that are traditionally associated with VOC emission from traffic-related sources (e.g., vehicle and aircraft exhaust) (Hoque et al., 2008). Traffic-related pollutants often exhibit a weekly concentration pattern attributed to higher activity on weekdays and lower activity on weekends (Baidar et al., 2015; Pollack et al., 2012). Factor 1 concentrations are lower on weekends in the current analysis (*Figure 8-2* a), building confidence in the assignment of a traffic-related source name. Factor 1 concentrations decrease with temperature from the beginning of the measurement campaign (July) to the end of the measurement campaign (October) consistent with the expected behavior of evaporative losses. The upwind westward direction of Factor 1 (Figure 8-3 a) also corresponds to the largest potential source of traffic-related emissions (two major freeways and central Redlands). This combined evidence suggests that Factor 1 may derive from the evaporation of liquid fuel from motor vehicles.

The highest absolute concentration in Factor 1 is methanol (red dot). Methanol is a component of gasoline, especially in high octane component blending (Methanol Institute, 2016). Even though methanol dominates Factor 1, < 2% of total methanol concentrations are associated with this factor. Other sources of methanol must be present at even higher concentrations upwind of Redlands.

It should be noted that factor 1 contains compounds not traditionally associated with traffic emissions. Other than BTEX and methanol, Factor 1 also contains relatively high amounts (> 20%) of Limonene, Propyl benzene, n-Butyl acetate, and parachlorobenzotrifluoride (PCBTF). Propyl benzene, n-Butyl acetate, and PCBTF (Gkatzelis et al., 2021a) are used as solvents for industrial printing or coating. Industrial solvents would naturally have a similar day-of-week profile as BTEX compounds. Limonene is a typical biogenic VOC tracer, but it can also be used as a fragrance in a variety of consumer products that would be used in urban areas (Gkatzelis et al., 2021a). Previous studies have determined that the time profiles of emissions from some VCP sources are similar to the time profile of traffic emissions (e.g., Benzene) (Coggon et al., 2018). This emissions co-linearity may lead to factor blending in the PMF analysis.

8.2.2 Factor 2: Petroleum fuel vapor

Factor 2 contains a large fraction of the measured Pentane, Butane, Butene, and Pentene. Notably, over 70% of Pentane is attributed to Factor 2. These alkanes and alkenes are components of gasoline blends, but the absence of BTEX compounds and the absence of strong day-of-week profile (*Figure 8-2* (b)) suggests that this factor is not a direct on-road traffic emission. These patterns suggest that Factor 2 may represent losses of gasoline vapor from the head space vapor in parked vehicle tanks, stationary fuel storage tanks, off-road gasoline engines, fuel distribution depots, or fuel refineries. Past studies also found divergent diurnal/weekly VOC emissions patterns from gasoline vapor and liquid fuel evaporation (Gentner et al., 2009; Guha et al., 2015), with lower time variation associated with gasoline vapor. It is notable that approximately 10% of the ethanol is contained in factor 2. This is consistent with the results from past studies in which mobile sources contribute less than 20% to the total ethanol in the Los Angeles atmosphere (McDonald et al., 2018).

The ratio of butane isomers and pentane isomers in the PMF factors may help constrain possible emissions sources. Branched isomers are slightly less volatile than straight chain isomers, but all isomers are affected by air mass mixing and have similar photochemical reactivities (Gilman et al., 2013). The (i/n) isomeric ratios in PMF Factor 2 are 0.53 for butane (iC_3/nC_3) and 1.2 for pentane (iC_5/nC_5). A previous study (Rossabi and Helmig, 2018) also measured $iC_3/nC_3 = 0.5$ in Los Angeles, which is consistent with iC_3/nC_3 in factor 2 of the current study. A value of iC_5/nC_5 $=2.45$ was measured in Pasadena, CA during CalNex-2010, which is higher than the ratio identified in factor 2 of the current study. Previous work (Gentner et al., 2009) found that the winter time liquid gasoline blend has $iC_5/nC_5 = 2.3$, and the summer time gasoline headspace vapor has iC_5/nC_5 $=3.96$. Gasoline-related sources should therefore have iC_5/nC_5 in range of 2.3~3.96., Measurements in Boulder, CO, found iC5/nC5=0.86, possibly due to the influence of oil and natural gas operations (Gilman 2013). This indicates that factor 2 in our PMF analysis might represent a mixture of multiple fuels and petroleum operations.

Figure *8-2* b suggests that Factor 2 concentrations decrease with temperature over the four-month measurement period. Factor 2 concentrations also increase in early October, possibly due to the changeover from summer-blend gasoline with lower Reid Vapor Pressure (RVP) to winter-blend gasoline with higher RVP. A fuel depot with 32 refined petroleum product tanks is located in Bloomington CA (~ 20 km upwind of the sampling site). The exact timing of the drawdown and refilling of these storage tanks is not known at this time. The wind rose for factor 2 (Figure 8-3b) suggests emission sources anywhere from the South through the West to the Northwest. The majority of the local gasoline stations, several large freight hubs, and a parking lot for school buses are all located to the West of the sampling site.

8.2.3 Factor 3: Blended Biogenic and Anthropogenic

Factor 3 contains a large fraction of p-Isopropyl Toluene (p-Cymene), and Limonene, both of which are terpenes that are emitted from biogenic sources (Kesselmeier and Staudt, 1999). Factor 3 concentrations decrease with ambient temperature in Redlands, with a correlation coefficient R = 0.58 (higher correlation with temperature than any other PMF Factor). Biogenic emissions have a strong temperature dependence (Guenther et al., 2006), building evidence that Factor 3 originates from a biogenic source. The CPF for Factor 3 is mainly from the West, which corresponds to the majority of the irrigated landscape in the immediate area around the sampling site.

Recent studies have found that anthropogenic sources (Coggon et al., 2021; Gkatzelis et al., 2021a; Pye et al., 2019) or urban landscaping (Gu et al., 2021) can also release significant amounts of terpenes in urban areas. Aside from terpenes, Factor 3 also contains large fractions of some alkanes, alkenes, and benzene, which are generally associated with anthropogenic sources. The majority of the irrigated landscape and population density are located in the same position in the current study region, which can cause similar concentration patterns for biogenic and anthropogenic compounds. PMF is known to blend factors with similar time series, suggesting that Factor 3 may represent contributions from both biogenic and anthropogenic sources.

8.2.4 Factor 4: VCP (Siloxane)

Factor 4 contains most of the D5-Siloxane and Isobutane concentrations. D5-Siloxanes have been reported as good tracers for personal care products (Coggon et al., 2018; Gkatzelis et al., 2021a). D5-Siloxanes have a long lifetime (typically 4~5 days in ambient conditions) and these compounds are widely used in personal care products. Isobutane is used in home cleaning and personal care products (Williams et al., 2017). Factor 4 also contains significant amounts of propylene, which is used in cooking fuel and personal care products.

The time series of Factor 4 concentrations does not exhibit a day-of-week trend or a seasonal trend that decreases with temperature. VOC emissions from personal care products are usually related to the population in urban areas (Coggon et al., 2021). Factor 4 concentrations increase upwards on a few days in September and October 2022, possibly due to the resumption of classes at nearby educational institutions approximately 1 km from the measurement site. The increasing population and personal care products usage from students could contribute to the increased VCP concentrations. The wind rose for Factor 4 (Figure 8-3 d) indicates a preferred source direction from the Northwest, consistent with the location of the University of Redlands and the greater City of Redlands.

8.2.5 Factor 5: University + K12 institutes chemicals

Factor 5 contains a large portion of the measured 1,4-Dichlorobenzene concentration, which may be used as a deodorant, as a disinfectant, in research laboratories, chemical manufacturing, and industrial cleaning. 1,4-Dichlorobenzene has also been found to be a tracer for insecticide (Gkatzelis et al., 2021a). Section 6.2 shows that 1,2-Dichlorobenzene and 1,4-Dichlorobenzene have similar seasonal trends, but PMF separates these two chemicals into individual factors. Therefore, only 1,4-Dichlorobenzene was used in the PMF analysis. Nearby educational institutions, commercial stores, and residential houses are all potential emission sources. The wind rose (Figure *8-3* (e)) indicates that Factor 5 has a preferred source directly to the South and broadly West. A middle school with over 1400 students is located 1 km to the South of the sampling site, and a high school with several thousand students is located 2.3 km to the West. It should be noted that winds from the south only occurred on approximately 6 days during the measurement period. The high CPF value in the southern direction for factor 5 does not indicate an exclusive source for this factor. Sources in the west and northwest direction are also indicated on the CPF plot for factor 5 (Figure *8-3* (e)).

8.2.6 Factor 6: Halogenated solvent

Factor 6 contains major contributions from halogenated compounds including Carbon tetrachloride, Dichloromethane, Trichloro-trifluoroethane, Dichlorotetrafluoroethane, and Trichlorofluoromethane. These halogenated compounds are commonly used as cleaning solvents in commercial laundry and dry-cleaning operations. A significant fraction of the Limonene concentration is also associated with Factor 6, likely due to its use as a fragrance in laundry detergents.

The emission of halogenated solvent could theoretically be influenced by both activity patterns and temperature. Factor 6 concentrations do not exhibit a strong seasonal trend, which may reflect the competing effects of decreasing temperature and increasing activity around the University of Redlands between July to October 2021.

The wind rose analysis indicates that the preferred source direction of Factor 6 is north of the measurement site. There are several dry cleaning and laundry locations in the region around the measurement site, with one location immediately to the north. Factor 6 may therefore reflect a localized source influence rather than a generalized regional source.

8.2.7 Factor 7: MeOH (decomposition of organic matter)

The dominant chemical signature in Factor 7 is Methanol (MeOH). Methanol is the second most abundant organic gas in the troposphere (Bates et al., 2021). The dominant source of atmospheric methanol is terrestrial plants, particularly during the growth and decay stages (Bates et al., 2021; Hu et al., 2011). The Factor 7 concentration time series follows a relatively stable background level punctuated by periods of concentration increases lasting 3-5 days. This pattern suggests that the methanol was emitted from multiple sources. One set of relatively uniform area sources contributes to the baseline concentrations while another point source contributes to peak concentrations. Waste composting emits large amounts of VOCs, in which alcohols (including methanol) constitute a major fraction (Kumar et al., 2011). Periodic cutting of tall grass or hay that is then left to dry could also potentially produce intermittent spikes in methanol concentrations.

The preferred source direction for Factor 7 is southwest and west of the measurement site (Figure 8-3 g). Air mass back trajectories were calculated starting at 11 AM local time on peak methanol days using the Hybrid Single-Particle Lagrangian Integrated Trajectory (HYSPLIT) model at an altitude of 500 m (Figure *8-4*). Air masses arrived from the Southwest or Southeast direction on those peak days. There is one landfill site in each of these directions and both of these landfills accept greenwaste organic matter. This suggests that composting emissions from landfills may contribute to Factor 7 concentration spikes.

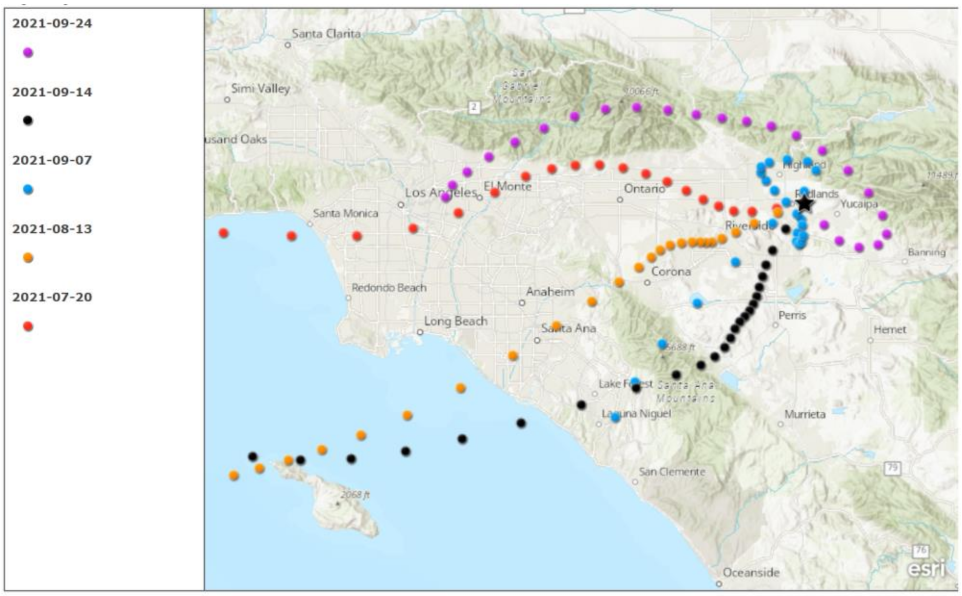

Esri, CGIAR, USGS | City of Anaheim, County of Los Angeles, California State Parks, Esri, HERE, Garmin, SafeGraph, FAO, METI/NASA, USGS, Bureau of Land Management, EPA, NPS

Figure 8-4 Airmass back trajectories starting at 11AM local time on peak methanol days calculated using the Hybrid Single-Particle Lagrangian Integrated Trajectory (HYSPLIT) model at an altitude of 500 m. Star indicates the sampling site, different color dots indicate the hourly location of the airmass back trajectory.

8.2.8 Factor 8: VCP (Ethanol)

The dominant chemical signature in Factor 8 is Ethanol with smaller contributions from D5-Siloxane, Limonene, Phenol, and p-Cymene. Ethanol is widely used in gasoline and personal care products, cleaning agents, and alcoholic beverages (Coggon et al., 2021; McDonald et al., 2018). Phenol can be used in painting products. D5-Siloxane and terpenes could be used in personal care products. The number of clear VCP compounds present in Factor 8 suggests that this factor is associated with VCPs. Approximately 80% of the total ethanol concentration was attributed to Factor 8 in the current study. This VCP contribution to ethanol is consistent with other recent studies. Coggon et al. (2021) used models to predict that VCPs contribute to 70% of the total ethanol concentration in New York City. Gkatzelis et al. (2021b) performed PMF analysis on PTR-MS measurements to determine that VCPs contribute to 83% of total ethanol concentrations in New York City. Past studies in Los Angeles found that mobile sources contribute less than 20% to total ethanol concentrations (McDonald et al., 2018), which is consistent with the results from the present study showing that the Gasoline Vapor Factor (Factor 2) contributes to approximately ~10% of the total ethanol concentration.

8.3 Associations between base-case chamber O_3 formation and PMF factors

The 3-hr base-case O_3 formation measured during each daily chamber experiment was used as a PMF input to identify associations between VOC sources and O_3 formation. Because O_3 is a secondary pollutant that has a non-linear relationship with precursor emissions, the O_3 'factor contribution' cannot be directly interpreted as a 'source contribution'. High O_3 loadings on a factor indicate that the conditions that produced high factor concentrations also produced high O_3 concentrations. The relationships between O_3 and the VOCs within that factor may not be causative, but instead, they may be driven by a common underlying mechanism.

Figure 8-5 shows the association between base-case chamber O_3 formation and each PMF VOC Factor. The VCP (Siloxane) Factor had the single highest association with O_3 formation at Redlands. Past modeling studies have predicted the importance of VCPs to O_3 formation in urban areas. Coggon et al. (2021) found that VCPs account for more than 50% of anthropogenic VOC (AVOC), which contributes ~20 ppb MDA8 O_3 concentration in New York City (NYC). Previous studies in Los Angeles (McDonald, 2018) also found that VCPs contribute to over 50% of the AVOC. Therefore, the high association between the VCP (Siloxane) Factor and O_3 formation could be due to similar VCP emission/formation patterns that contribute to O_3 formation in urban areas.

The Biogenic Factor had the second highest association with O_3 formation. The Biogenic Factor concentrations increase with temperature and solar radiation due to the nature of biogenic VOC emissions. These same conditions encourage O_3 formation. Recent studies (Wu et al, 2022) in Sacramento found that the seasonal pattern of O_3 formation is consistent with a strong biogenic VOC contribution. Sacramento is a city with considerably more tree cover than the SoCAB. Redlands is in the downwind portion of the SoCAB that has many large and diverse upwind sources contributing to a complex VOCs composition, but biogenic sources still appear to be associated with high O_3 formation at this location.

The Halogenated Solvents Factor had a strong association with chamber O_3 formation that was comparable to the biogenic factor in the current study. However, the dominant chemicals (e.g., Carbon tetrachloride, Dichloromethane, etc.) in the Halogenated Solvent Factor have very low Ozone formation potential. The Halogenated Solvents Factor does contain limonene, which has high O_3 formation potential. It is possible that additional chemicals similar to limonene are emitted along with this factor, but were not measured in the current study. Recall that the Halogenated Solvent Factor was determined to be a local source rather than a general area source, and so this factor may not make significant contributions to O_3 formation at Redlands during non-stagnant atmospheric conditions.

The VCP (Ethanol) Factor had the fourth highest association with chamber O_3 formation, closely followed by the Factor 2 (Petroleum fuel vapor). Past studies identified emissions from mobile sources as the leading cause of O_3 formation in Southern California, since vehicles released large amounts of both precursor NO_x and VOCs. The chamber measurements suggest that Redlands is mostly in the NO_x-rich chemical regime during relatively lower-O_3 concentration days, but NO_x-limited during relatively higher O_3 concentration days. Therefore, higher NO_x may lead to lower O_3 concentration on average, but reducing NO_x is still necessary to avoid extreme O_3 events until the atmospheric chemistry transitions completely to the NOx-limited regime. This non-linear relationship between O_3 and its precursor may dampen the association between O_3 formation and the Gasoline Evaporation Loss Factor in the current study.

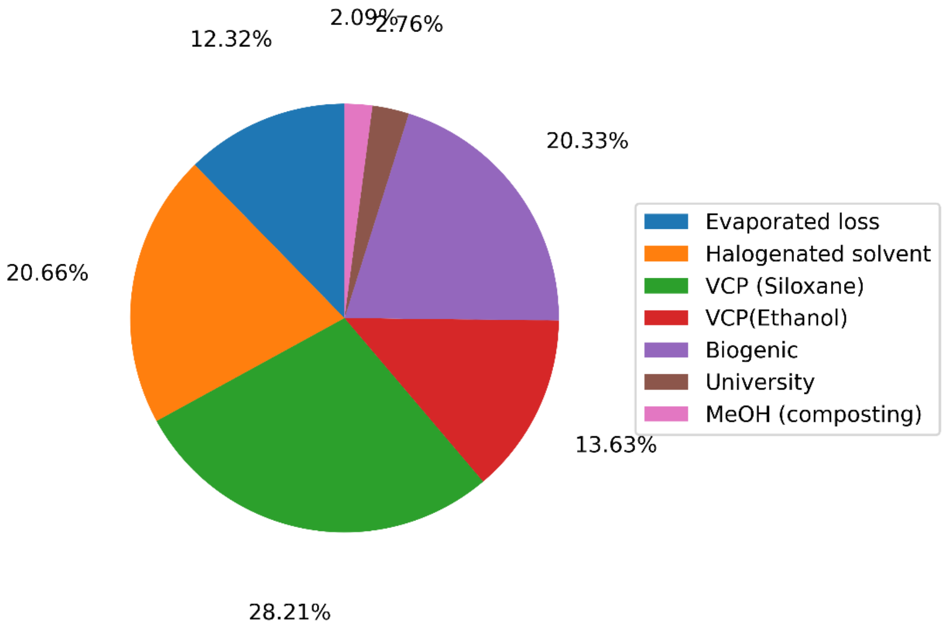

Figure 8-5 Association between base-case chamber O_3 formation and each PMF factor averaged across the entire sampling period. Gasoline vapor is not shown because it has no association.

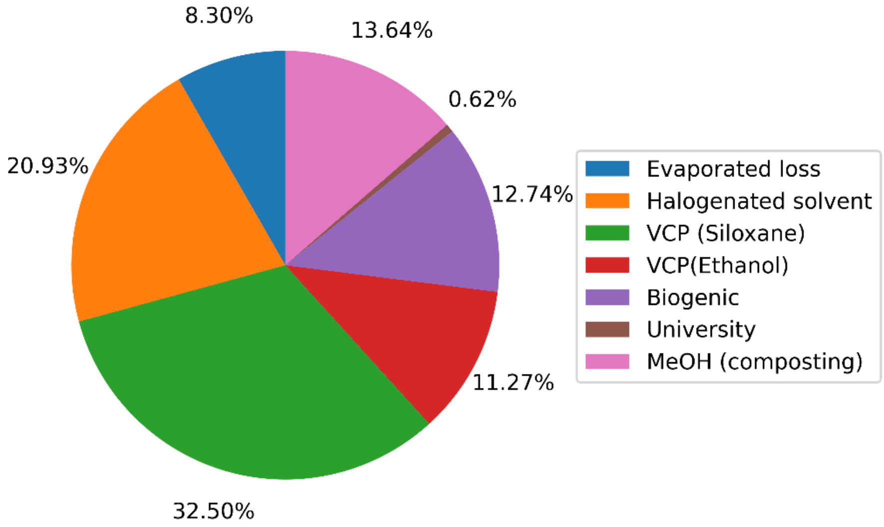

Figure 8-6 Association between base-case chamber O_3 formation and each PMF factor on NOx-rich days.

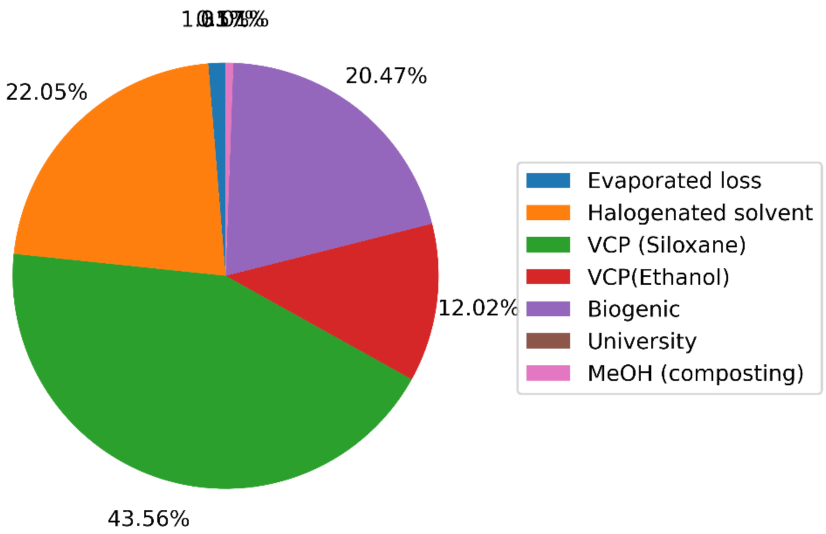

Figure 8-7 Association between base-case chamber O3 formation and each PMF factor on NOx-limited days.

The associations discussed in the current study convey useful information, but they are not necessarily causative. To emphasize this point, the Ozone formation potential (OFP) was calculated for each PMF factor by summing up the mixing ratio of each VOC species in that factor multiplied by its maximum incremental reactivity (MIR). The weighted OFP for each factor (Table *8-2*) suggests that MeOH (decomposition of organic matter) should have the highest direct OFP, but the PMF analysis demonstrates that days with high methanol concentrations are not days with high O_3 formation. The ‘factor contribution’ to O_3 formation reflects a range of chemical and meteorological effects that indicate associations rather than causation.

Table 8-2 Ozone formation potential (OPF) for each PMF-resolved factor

Factor name	University	Gasoline vapor	Biogenic	VCP (Ethanol)	Halogenated solvent	Evaporated loss	MeOH (composting)	VCP (Siloxane)
MIR (ppb)	2.67	3.26	1.33	11.61	6.35	2.62	85.10	4.93

9 CONCLUSIONS

VOC measurements at Redlands California identified 95 compounds at concentrations above detection limits between July 10, 2021, to November 01, 2021, as part of the RECAP field campaign. Major compound classes characterized by the measurements include halocarbons and volatile organics, aldehydes and ketones, alcohols and phenols, semi-volatile organic compounds, total organic silicon, and terpenes. The majority of the VOC concentrations follow an expected log-normal concentration profile. Time trends are apparent in many VOC concentrations corresponding to seasonal temperature patterns, day-of-week patterns, and seasonal activity patterns that would be expected for nearby sources. Terpenes underwent a seasonal cycle of declining concentrations as summer progressed towards fall, punctuated by high concentrations events that may be associated with the periodic cutting of grasses or hay. Compounds within the BTEX category had a strong day of week pattern and a strong seasonal pattern, suggesting that temperature strongly influenced evaporative emissions from motor vehicles. Several halogenated compounds and assorted volatile chemical products had markedly increased concentrations starting in the fall season when classes were expected to resume at the nearby University of Redlands.

Positive Matrix Factorization (PMF) analysis identified eight VOC factors with preliminary source names recognized as (i) evaporation of liquid motor vehicle fuel, (ii) escape of vapors from the headspace of petroleum storage tanks, (iii) biogenics, (iv) volatile chemical products (VCPs) associated with siloxanes, (v) University and K12 institutional chemicals, (vi) halogenated solvents, (vii) methanol with contributions from gasoline and composting, and (viii) ethanol derived from VCPs. O_3 formation was most strongly associated with the VCP (siloxane), biogenic, halogenated solvents, VCP (ethanol), and gasoline evaporation at the Redlands location, in order of decreasing importance. The ranking of these associations does not match the ranking of the calculated O_3 formation potential for each factor, indicating that associations may be driven by underlying mechanisms.

10 FUTURE WORK

Future work should be conducted to further understand the underlying mechanisms that cause high associations between O_3 formation and VOC factors at the Redlands monitoring site. The measurements made in the current field project should also be compared to predictions from chemical transport models (CTMs) that calculate O_3 source contributions using tagging methods.

11 REFERENCES

2B Technologies: Ozone Monitor Operation Manual (Model 205)., 2018.

Baidar, S., Hardesty, R. M., Kim, S. W., Langford, A. O., Oetjen, H., Senff, C. J., Trainer, M. and Volkamer, R.: Weakening of the weekend ozone effect over California's South Coast Air Basin, Geophys. Res. Lett., 42(21), 9457–9464, doi:10.1002/2015GL066419, 2015.

Bates, K. H., Jacob, D. J., Wang, S., Hornbrook, R. S., Apel, E. C., Kim, M. J., Millet, D. B., Wells, K. C., Chen, X., Brewer, J. F., Ray, E. A., Commane, R., Diskin, G. S. and Wofsy, S. C.: The Global Budget of Atmospheric Methanol: New Constraints on Secondary, Oceanic, and Terrestrial Sources, J. Geophys. Res. Atmos., 126(4), e2020JD033439, doi:10.1029/2020JD033439, 2021.

Brown, S. G., Frankel, A. and Hafner, H. R.: Source apportionment of VOCs in the Los Angeles area using positive matrix factorization, Atmos. Environ., 41(2), 227–237, doi:10.1016/j.atmosenv.2006.08.021, 2007.

Cahill, T. M.: Ambient acrolein concentrations in coastal, remote, and urban regions in California, Environ. Sci. Technol., 48(15), 8507–8513, doi:10.1021/ES5014533/SUPPL_FILE/ES5014533_SI_001.PDF, 2014.

California Energy Commision: Petroleum Watch. [online] Available from: https://www.energy.ca.gov/sites/default/files/2020-12/2020-11 Petroleum Watch_ADA.pdf#page=1&zoom=100,46,2270, 2020.

Chossière, G. P., Xu, H., Dixit, Y., Isaacs, S., Eastham, S. D., Allroggen, F., Speth, R. L. and Barrett, S. R. H.: Air pollution impacts of COVID-19–related containment measures, Sci. Adv., 7(21), doi:10.1126/SCIADV.ABE1178, 2021.

Coggon, M. M., McDonald, B. C., Vlasenko, A., Veres, P. R., Bernard, F., Koss, A. R., Yuan, B., Gilman, J. B., Peischl, J., Aikin, K. C., Durant, J., Warneke, C., Li, S. M. and De Gouw, J. A.: Diurnal Variability and Emission Pattern of Decamethylcyclopentasiloxane (D5) from the Application of Personal Care Products in Two North American Cities, Environ. Sci. Technol., 52(10), 5610–5618, doi:10.1021/ACS.EST.8B00506, 2018.

Coggon, M. M., Gkatzelis, G. I., McDonald, B. C., Gilman, J. B., Schwantes, R. H., Abuhassan, N., Aikin, K. C., Arendd, M. F., Berkoff, T. A., Brown, S. S., Campos, T. L., Dickerson, R. R., Gronoff, G., Hurley, J. F., Isaacman-Vanwertz, G., Koss, A. R., Li, M., McKeen, S. A., Moshary, F., Peischl, J., Pospisilova, V., Ren, X., Wilson, A., Wu, Y., Trainer, M. and Warneke, C.: Volatile chemical product emissions enhance ozone and modulate urban chemistry, Proc. Natl. Acad. Sci. U. S. A., 118(32), doi:10.1073/pnas.2026653118, 2021.

Coggona, M. M., Gkatzelis, G. I., McDonald, B. C., Gilman, J. B., Schwantes, R. H., Abuhassan, N., Aikin, K. C., Arendd, M. F., Berkoff, T. A., Brown, S. S., Campos, T. L., Dickerson, R. R., Gronoff, G., Hurley, J. F., Isaacman-Vanwertz, G., Koss, A. R., Li, M., McKeen, S. A., Moshary, F., Peischl, J., Pospisilova, V., Ren, X., Wilson, A., Wu, Y., Trainer, M. and Warneke, C.: Volatile chemical product emissions enhance ozone and modulate urban chemistry, Proc. Natl. Acad. Sci. U. S. A., 118(32), doi:10.1073/pnas.2026653118, 2021.

Cooper, M. J., Martin, R. V, Hammer, M. S., Levelt, P. F., Veefkind, P., Lamsal, L. N., Krotkov, N. A., Brook, J. R. and Mclinden, C. A.: Global fine-scale changes in ambient NO 2 during COVID-19 lockdowns, 380 | Nat. |, 601, doi:10.1038/s41586-021-04229-0, 2022.

Gentner, D. R., Harley, R. A., Miller, A. M. and Goldstein, A. H.: Diurnal and seasonal variability of gasoline-related volatile organic compound emissions in Riverside, California, Environ. Sci. Technol., 43(12), 4247–4252, doi:10.1021/ES9006228/SUPPL_FILE/ES9006228_SI_001.PDF, 2009.

Gilman, J. B., Lerner, B. M., Kuster, W. C. and De Gouw, J. A.: Correction to Source Signature of Volatile Organic Compounds from Oil and Natural Gas Operations in Northeastern Colorado, Environ. Sci. Technol., 47(17), 10094, doi:10.1021/ES4036978, 2013.

Gkatzelis, G. I., Coggon, M. M., McDonald, B. C., Peischl, J., Aikin, K. C., Gilman, J. B., Trainer, M.

and Warneke, C.: Identifying Volatile Chemical Product Tracer Compounds in U.S. Cities, Environ. Sci. Technol., 55(1), 188–199, doi:10.1021/acs.est.0c05467, 2021a.

Gkatzelis, G. I., Coggon, M. M., McDonald, B. C., Peischl, J., Gilman, J. B., Aikin, K. C., Robinson, M. A., Canonaco, F., Prevot, A. S. H., Trainer, M. and Warneke, C.: Observations Confirm that Volatile Chemical Products Are a Major Source of Petrochemical Emissions in U.S. Cities, Environ. Sci. Technol., 55(8), 4332–4343, doi:10.1021/ACS.EST.0C05471, 2021b.

Gu, S., Guenther, A. and Faiola, C.: Effects of Anthropogenic and Biogenic Volatile Organic Compounds on Los Angeles Air Quality, Environ. Sci. Technol., 55(18), 12191–12201, doi:10.1021/ACS.EST.1C01481/ASSET/IMAGES/LARGE/ES1C01481_0004.JPEG, 2021.

Guenther, A., Karl, T., Harley, P., Wiedinmyer, C., Palmer, P. I. and Geron, C.: Estimates of global terrestrial isoprene emissions using MEGAN (Model of Emissions of Gases and Aerosols from Nature), Atmos. Chem. Phys., 6(11), 3181–3210, doi:10.5194/acp-6-3181-2006, 2006.

Guha, A., Gentner, D. R., Weber, R. J., Provencal, R. and Goldstein, A. H.: Source apportionment of methane and nitrous oxide in California's San Joaquin Valley at CalNex 2010 via positive matrix factorization, Atmos. Chem. Phys., 15(20), 12043–12063, doi:10.5194/ACP-15-12043-2015, 2015.

He, Z., Wang, X., Ling, Z., Zhao, J., Guo, H., Shao, M. and Wang, Z.: Contributions of different anthropogenic volatile organic compound sources to ozone formation at a receptor site in the Pearl River Delta region and its policy implications, Atmos. Chem. Phys., 19(13), 8801–8816, doi:10.5194/ACP-19-8801-2019, 2019.

Hoque, R. R., Khillare, P. S., Agarwal, T., Shridhar, V. and Balachandran, S.: Spatial and temporal variation of BTEX in the urban atmosphere of Delhi, India, Sci. Total Environ., 392(1), 30–40, doi:10.1016/J.SCITOTENV.2007.08.036, 2008.

Hu, L., Millet, D. B., Mohr, M. J., Wells, K. C., Griffis, T. J. and Helmig, D.: Sources and seasonality of atmospheric methanol based on tall tower measurements in the US Upper Midwest, Atmos. Chem. Phys., 11(21), 11145–11156, doi:10.5194/ACP-11-11145-2011, 2011.

Karavalakis, G., Short, D., Vu, D., Russell, R., Hajbabaei, M., Asa-Awuku, A. and Durbin, T. D.: Evaluating the Effects of Aromatics Content in Gasoline on Gaseous and Particulate Matter Emissions from SI-PFI and SIDI Vehicles, , doi:10.1021/es5061726, 2015.

Kesselmeier, J. and Staudt, M.: Biogenic Volatile Organic Compounds (VOC): An Overview on Emission, Physiology and Ecology, J. Atmos. Chem. 1999 331, 33(1), 23–88, doi:10.1023/A:1006127516791, 1999.

Kim, E., Hopke, P. K., Larson, T. V. and Covert, D. S.: Analysis of Ambient Particle Size Distributions Using Unmix and Positive Matrix Factorization, Environ. Sci. Technol., 38(1), 202–209, doi:10.1021/es030310s, 2004.

Kumar, A., Alaimo, C. P., Horowitz, R., Mitloehner, F. M., Kleeman, M. J. and Green, P. G.: Volatile organic compound emissions from green waste composting: Characterization and ozone formation, Atmos. Environ., 45(10), 1841–1848, doi:10.1016/J.ATMOSENV.2011.01.014, 2011.

Ling, Z. H., Guo, H., Cheng, H. R. and Yu, Y. F.: Sources of ambient volatile organic compounds and their contributions to photochemical ozone formation at a site in the Pearl River Delta, southern China, Environ. Pollut., 159(10), 2310–2319, doi:10.1016/J.ENVPOL.2011.05.001, 2011.

Liu, J., Lipsitt, J., Jerrett, M. and Zhu, Y.: Decreases in Near-Road NO and NO2Concentrations during the COVID-19 Pandemic in California, Environ. Sci. Technol. Lett., (2), doi:10.1021/acs.estlett.0c00815, 2020.

Lu, Q., N. Murphy, B., Qin, M., J. Adams, P., Zhao, Y., O. T. Pye, H., Efstathiou, C., Allen, C. and L. Robinson, A.: Simulation of organic aerosol formation during the CalNex study: Updated mobile emissions and secondary organic aerosol parameterization for intermediate-volatility organic compounds, Atmos. Chem. Phys., 20(7), 4313–4332, doi:10.5194/ACP-20-4313-2020, 2020.

McDonald, B. C., De Gouw, J. A., Gilman, J. B., Jathar, S. H., Akherati, A., Cappa, C. D., Jimenez, J. L., Lee-Taylor, J., Hayes, P. L., McKeen, S. A., Cui, Y. Y., Kim, S. W., Gentner, D. R., Isaacman-VanWertz, G., Goldstein, A. H., Harley, R. A., Frost, G. J., Roberts, J. M., Ryerson, T. B. and Trainer, M.: Volatile chemical products emerging as largest petrochemical source of urban organic emissions, Science (80-.).,

359(6377), 760–764, doi:10.1126/science.aaq0524, 2018.
Methanol Institute: Methanol Use in Gasoline. Blending, Storage and Handling of Gasoline Containing Methanol Methanol, , 740, 30, 2016.
Montzka, S. A., Dutton, G. S., Yu, P., Ray, E., Portmann, R. W., Daniel, J. S., Kuijpers, L., Hall, B. D., Mondeel, D., Siso, C., Nance, J. D., Rigby, M., Manning, A. J., Hu, L., Moore, F., Miller, B. R. and Elkins, J. W.: An unexpected and persistent increase in global emissions of ozone-depleting CFC-11, Nat. 2018 5577705, 557(7705), 413–417, doi:10.1038/s41586-018-0106-2, 2018.
New Jersey Department of Environmental Protection: BACKGROUND LEVELS OF VOLATILE ORGANIC CHEMICALS IN HOMES: A REVIEW OF RECENT LITERATURE. [online] Available from: https://www.nj.gov/dep/srp/guidance/vaporintrusion/vig_background_levels_of_vos.pdf (Accessed 18 August 2022), 2016.
Park, S., Western, L. M., Saito, T., Redington, A. L., Henne, S., Fang, X., Prinn, R. G., Manning, A. J., Montzka, S. A., Fraser, P. J., Ganesan, A. L., Harth, C. M., Kim, J., Krummel, P. B., Liang, Q., Mühle, J., O'Doherty, S., Park, H., Park, M. K., Reimann, S., Salameh, P. K., Weiss, R. F. and Rigby, M.: A decline in emissions of CFC-11 and related chemicals from eastern China, Nat. 2021 5907846, 590(7846), 433–437, doi:10.1038/s41586-021-03277-w, 2021.
Parrish, D. D., Xu, J., Croes, B. and Shao, M.: Air quality improvement in Los Angeles—perspectives for developing cities, Front. Environ. Sci. Eng., 10(5), doi:10.1007/s11783-016-0859-5, 2016.
Pollack, I. B., Ryerson, T. B., Trainer, M., Parrish, D. D., Andrews, A. E., Atlas, E. L., Blake, D. R., Brown, S. S., Commane, R., Daube, B. C., De Gouw, J. A., Dubé, W. P., Flynn, J., Frost, G. J., Gilman, J. B., Grossberg, N., Holloway, J. S., Kofler, J., Kort, E. A., Kuster, W. C., Lang, P. M., Lefer, B., Lueb, R. A., Neuman, J. A., Nowak, J. B., Novelli, P. C., Peischl, J., Perring, A. E., Roberts, J. M., Santoni, G., Schwarz, J. P., Spackman, J. R., Wagner, N. L., Warneke, C., Washenfelder, R. A., Wofsy, S. C. and Xiang, B.: Airborne and ground-based observations of a weekend effect in ozone, precursors, and oxidation products in the California South Coast Air Basin, J. Geophys. Res. Atmos., 117(3), 1–14, doi:10.1029/2011JD016772, 2012.
Pye, H. O. T., D'Ambro, E. L., Lee, B. H., Schobesberger, S., Takeuchi, M., Zhao, Y., Lopez-Hilfiker, F., Liu, J., Shilling, J. E., Xing, J., Mathur, R., Middlebrook, A. M., Liao, J., Welti, A., Graus, M., Warneke, C., de Gouw, J. A., Holloway, J. S., Ryerson, T. B., Pollack, I. B. and Thornton, J. A.: Anthropogenic enhancements to production of highly oxygenated molecules from autoxidation, Proc. Natl. Acad. Sci. U. S. A., 116(14), 6641–6646, doi:10.1073/PNAS.1810774116, 2019.
Van Rooy, P., Tasnia, A., Barletta, B., Buenconsejo, R., Crounse, J. D., Kenseth, C., Meinardi, S., Murphy, S., Parker, H., Schulze, B., Seinfeld, J. H., Wennberg, P. O., Blake, D. R. and Barsanti, K. C.: Observations of Volatile Organic Compounds in the Los Angeles Basin during COVID-19, ACS Earth Sp. Chem., doi:10.1021/acsearthspacechem.1c00248, 2021.
Rossabi, S. and Helmig, D.: Changes in Atmospheric Butanes and Pentanes and Their Isomeric Ratios in the Continental United States, J. Geophys. Res. Atmos., 123(7), 3772–3790, doi:10.1002/2017JD027709, 2018.
Scheutz, C., Winther, K. and Kjeldsen, P.: Removal of halogenated organic compounds in landfill gas by top covers containing zero-valent iron, Environ. Sci. Technol., 34(12), 2557–2563, doi:10.1021/ES991301F/ASSET/IMAGES/LARGE/ES991301FF00005.JPEG, 2000.
Simpson, I. J., Blake, D. R., Blake, N. J., Meinardi, S., Barletta, B., Hughes, S. C., Fleming, L. T., Crawford, J. H., Diskin, G. S., Emmons, L. K., Fried, A., Guo, H., Peterson, D. A., Wisthaler, A., Woo, J.-H., Barré, J., Gaubert, B., Kim, J., Kim, M. J., Kim, Y., Knote, C., Mikoviny, T., Pusede, S. E., Schroeder, J. R., Wang, Y., Wennberg, P. O. and Zeng, L.: Characterization, sources and reactivity of volatile organic compounds (VOCs) in Seoul and surrounding regions during KORUS-AQ, Elem. Sci. Anthr., 8, doi:10.1525/ELEMENTA.434, 2020.
U.S. Environmental Protection Agency: Compendium Method TO-17: Determination of Volatile Organic Compounds in Ambient Air Using Active Sampling Onto Sorbent Tubes., 1999a.
U.S. Environmental Protection Agency: Method TO-11A: Compendium of Methods for the Determination of Toxic Organic Compounds in Ambient Air Second Edition Compendium Method TO-

11A Determination of Formaldehyde in Ambient Air Using Adsorbent Cartridge Followed by High Performance Liquid Chromat., 1999b.
U.S. Environmental Protection Agency: EPA Positive M atrix Factorization (PMF) 5.0 Fundamentals and User Guide, Washington, DC 20460., 2014.
Warneke, C., De Gouw, J. A., Holloway, J. S., Peischl, J., Ryerson, T. B., Atlas, E., Blake, D., Trainer, M., Parrish, D. D., Warneke, C. :, De Gouw, J. A., Holloway, J. S., Peischl, J., Ryerson, T. B., Atlas, E., Blake, D., Trainer, M. and Parrish, D. D.: Multiyear trends in volatile organic compounds in Los Angeles, California: Five decades of decreasing emissions, J. Geophys. Res. Atmos., 117(D21), 0–17, doi:10.1029/2012JD017899, 2012.
Williams, A. J., Grulke, C. M., Edwards, J., McEachran, A. D., Mansouri, K., Baker, N. C., Patlewicz, G., Shah, I., Wambaugh, J. F., Judson, R. S. and Richard, A. M.: The CompTox Chemistry Dashboard: A community data resource for environmental chemistry, J. Cheminform., 9(1), doi:10.1186/S13321-017-0247-6, 2017.
Wu, S., Lee, H. J., Anderson, A., Liu, S., Kuwayama, T., Seinfeld, J. H. and Kleeman, M. J.: Direct measurements of ozone response to emissions perturbations in California, Atmos. Chem. Phys., 22(7), 4929–4949, doi:10.5194/acp-22-4929-2022, 2022.
Xie, Y. and Berkowitz, C. M.: The use of positive matrix factorization with conditional probability functions in air quality studies: An application to hydrocarbon emissions in Houston, Texas, Atmos. Environ., 40(17), 3070–3091, doi:10.1016/J.ATMOSENV.2005.12.065, 2006.
Zhang, Q., Jimenez, J. L., Canagaratna, M. R., Ulbrich, I. M., Ng, N. L., Worsnop, D. R. and Sun, Y.: Understanding atmospheric organic aerosols via factor analysis of aerosol mass spectrometry: A review, Anal. Bioanal. Chem., 401(10), 3045–3067, doi:10.1007/s00216-011-5355-y, 2011.